MONASH MOTORSPORT

FINAL YEAR THESIS COLLECTION

Design and Manufacture of an SLS Printed Intake Using ETC for FSAE

Samuel Wilson - 2019

The Final Year Thesis is a technical engineering assignment undertaken by students of Monash University. Monash Motorsport team members often choose to conduct this assignment in conjunction with the team.

The theses shared in the Monash Motorsport Final Year Thesis Collection are just some examples of those completed.

These theses have been the cornerstone for much of the team's success. We would like to thank those students that were not only part of the team while at university but also contributed to the team through their Final Year Thesis.

The purpose of the team releasing the Monash Motorsport Final Year Thesis Collection is to share knowledge and foster progress in the Formula Student and Formula-SAE community.

We ask that you please do not contact the authors or supervisors directly, instead for any related questions please email info@monashmotorsport.com

DESIGN AND MANUFACTURE OF AN SLS PRINTED INTAKE USING ETC FOR FSAE

SAMUEL JOEL WILSON (27857719)

SUPERVISED BY: DR. SCOTT WORDLEY

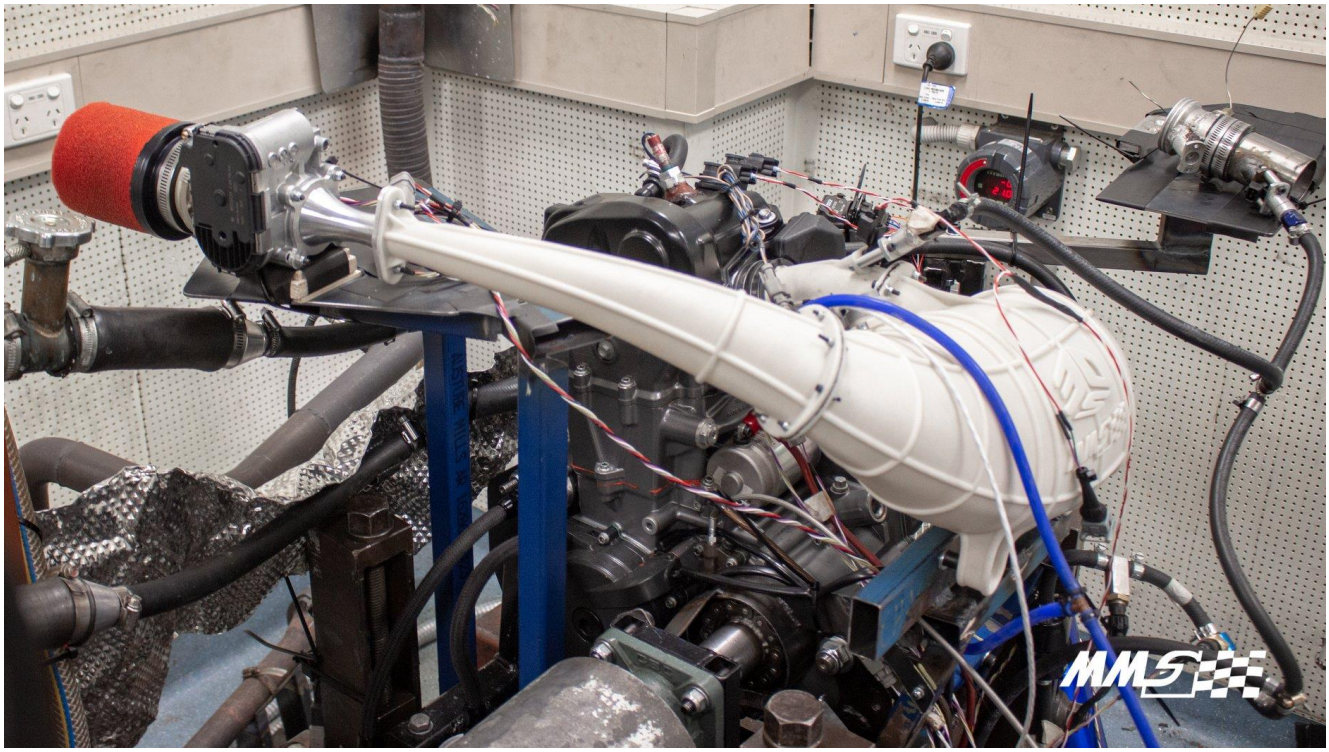

SUMMARY

Using a point simulator and analysis of previous results, Monash Motorsport (MMS) has elected to use a KTM 690 Duke R in its 2019 combustion car, M19-C. For the car to achieve a high concept utilisation at competition (ratio of points scoring potential of the car to actual points scored), maximising the power output of the engine and increasing its efficiency is critical. Based on limitations found with the 2018 intake system, the decision was made to utilise SLS 3D printing for intake system production to harness the advantages of virtually unlimited geometrical freedom and reduce manufacturing time and to utilise Electronic Throttle Control (ETC) in preference to a mechanical throttle. This report focuses on maximising the performance of the KTM 690 Duke R, and M19-C, through intake system analysis, simulation and design.

It has been identified that one of the key influences on the volumetric efficiency of an engine is the intake system design, (Norizan et al., 2014) and that the development of a high-performing intake system relies on acquiring and analysing relevant data (Kariotakis, 2011). Previous dynamometer testing and simulation allowed for the selection of geometrical parameters prior to design and removed the need to produce a modular, 'test intake' as has been required previously. This previous data and simulation showed that a runner length of 220mm and a plenum volume of 6 litres should be chosen.

Surface-driven CAD, Finite Element Analysis (FEA), Computational Fluid Dynamics (CFD) and Ricardo 1D engine simulation were all used during the design of the intake. This was necessary to utilise the geometrical freedom offered by the SLS 3D printing method. Ricardo confirmed that through the removal of sudden changes in direction and cross-sectional area, the pressure losses through the intake system could be minimised and power and efficiency increased as a result. Surfacing CAD was then used to realise the smooth geometry, and FEA used to guide the structure of the system to minimise mass while meeting stress and deflection targets. Steady-state CFD was attempted on the throttle, restrictor and diffuser but was not largely influential in the design, due to difficulty with meshing and convergence. The design process resulted in a plenum volume of 6 litres and a runner length of 200mm, with the runner length slightly shortened from target for packaging reasons.

The intake system was then installed and calibrated on the Monash in-house dynamometer, where fuel and ignition tables were calibrated, and fuel injector selection undertaken. The Bosch 32mm Electronic Throttle Body (ETB) was also calibrated and data gathered to assist in the creation of the throttle profile. Here, a peak power of 48.6 kW was observed at 8500 RPM and a peak torque of 62.2 Nm at 6000 RPM, representing deltas of 1.5 kW and 2 Nm compared to the 2018 intake system.

The system was then installed on M19-C and has performed without fault for over 700km of driving in all weather conditions. Some shortcomings have been realised, and the recommended solutions for these are documented in this report. Data analysis of the system and combustion powertrain as a whole is ongoing to validate and quantify performance compared to M18-C, and physical testing was carried out to validate and calibrate the FEA model. Further refinement of the CFD model was undertaken and recommendations with regards to its use made.

TABLE OF CONTENTS

TABLE OF FIGURES

1. INTRODUCTION

Formula-SAE (F-SAE) is the largest international university design competition in the world. Student teams design, manufacture, test and compete with formula-style vehicles across a range of dynamic and static events, vying for a total of 1000 points (Society of Automotive Engineers, 2019). The static events include cost & manufacturing, business presentation and engineering design, while dynamic events include acceleration, skid pad, autocross and endurance. There are three classes of vehicle permitted in the competition; combustion, electric and driverless, with the former two competing in the events described above and the driverless competing in a modified version of the competition. M17-C and M18-C competed through 2017 and 2018 across a range of events in Australia and Europe and are the most successful Monash Motorsport (MMS) combustion cars to date.

The purpose of an intake system in a combustion engine is to provide clean air to the engine, and, except for direct-injection and diesel engines, facilitate the mixing of the air-fuel mixture prior to entering the combustion chamber. In F-SAE a restrictor is mandated by rules (20mm for 98-RON fuelled vehicles and 19mm for E85) to limit airflow to the engine and therefore limit power output. The restrictor also dictates much of the intake design, as designing a restricted intake carries different challenges and limitations than for a regular, non-restricted intake.

Figure 1: The 2018 F-SAE combustion vehicle from MMS, M18-C (Monash Motorsport, 2018)

The main components of an intake system in F-SAE are; the throttle body, restrictor, diffuser, plenum and runner. The throttle body controls the amount of air flow into the intake system and therefore into the engine, the restrictor restricts the maximum airflow into the system and the diffuser gradually diffuses the air that passes through the restrictor to recover static pressure. The plenum acts as ‘air storage’ which the engine draws from during the intake stroke. Finally, the runner transports air from the plenum to the engine and its length is chosen to take advantage of resonance effects. All these components should be designed to work together to minimise pressure loss through the system and mitigate the effects of the restrictor as much as possible.

M18-C was powered by a 2017 KTM 690 Duke-R single cylinder engine, with a naturally aspirated intake system primarily fabricated from aluminium using a mechanical throttle body. The engine was controlled by a MoTeC M400 ECU that had been in use by the team since 2010. The MoTeC M150, which is an updated ECU with increased functionality over the M400, has been purchased for use in 2019. The M19-C will be using the same powertrain concept as the M18-C and thus the data gained over the last two years can be utilised to direct design decisions of the intake system.

The main limitations identified from M18-C's intake system stem from its aluminium construction. This includes only being able to achieve simple shapes and geometry, causing sudden changes in cross sectional area which produces pressure losses. The simple geometry also reduces the utilisation of the envelope that the intake is placed in. Inversely, using selective laser sintering (SLS) to produce the intake allows the utilisation of organic shapes and smooth cross-sectional area changes to counteract the limitations stated above. Finally, the use of SLS will greatly reduce manufacturing man-hours compared to fabricating an aluminium intake.

An electronic throttle body (ETB) has been selected in preference to a traditional mechanical throttle body. In conjunction with using the M150, this allows for the implementation of electronic throttle control (ETC). ETC has only become an allowable form of throttle control in F-SAE since 2015 (Society of Automotive Engineers, 2015). ETC offers many advantages over traditional throttle control, primarily in tunability and usability. Launch control can be implemented through throttle position rather than ignition cut, allowing the wheels to stay closer to the target slip ratio and increasing longitudinal acceleration. Custom throttle valve to pedal position maps can be set for different drivers and different events, which is particularly important in an event such as skid pad, where driving at a steady state on the limit of grip is crucial to setting a good time. Idle position can be set into the throttle body, starting can be done by varying throttle position, noise tests can be simplified, and the throttle cable is no longer needed.

2. LITERATURE REVIEW

2.1 The Four Stroke Engine

In the F-SAE competition, rule IC1.1.1 states: "The engine(s) used to power the vehicle must: a. Be a piston engine(s) using a four-stroke primary heat cycle…" (Society of Automotive Engineers, 2019). In a four-stroke engine, each engine cycle consists of four strokes; intake, compression, power and exhaust. These occur over two revolutions of the crankshaft.

Intake: The intake stroke begins with the piston at Top Dead Centre (TDC), after which it descends. The intake valve is also opened, and the low pressure created by the moving piston, and hence increasing cylinder volume, causes the intake charge (fuel and air mixture) to flow into the cylinder.

Compression: The compression stroke begins with the piston at Bottom Dead Centre (BDC), after which it ascends and reduces cylinder volume. The intake and exhaust valves are closed, and hence the intake charge is compressed as the piston approaches TDC.

Power: Just before the piston reaches TDC, the spark plug will ignite the intake charge, causing combustion and a large pressure increase within the cylinder. This causes the cylinder to be pushed back down towards BDC with force, and outputs power through the crankshaft.

Exhaust: As the piston travels up from BDC after the power stroke, the exhaust valve will open. The positive pressure inside the cylinder from combustion and the upwards movement of the piston causes the exhaust gases to flow out of the cylinder. The cycle then repeats.

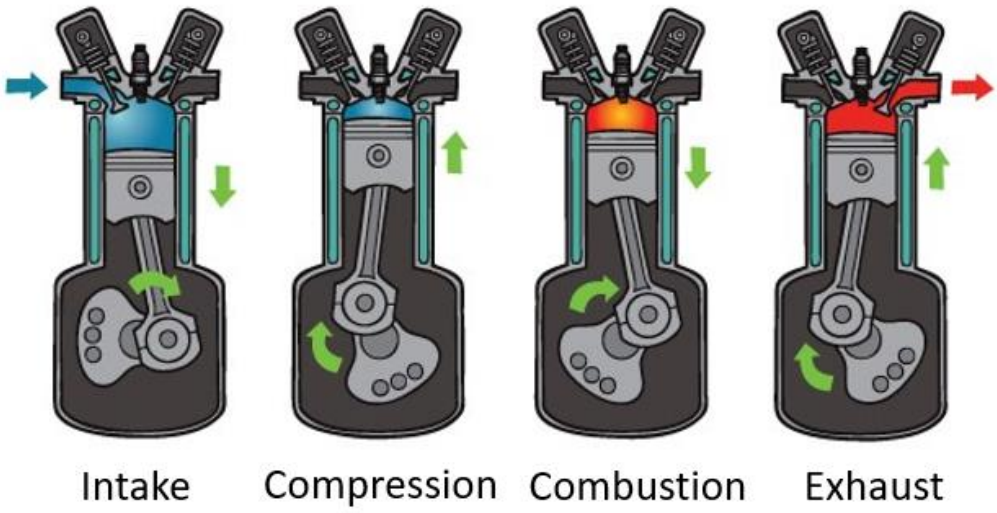

Figure 2: 4-stroke engine cycle (MechStuff, 2018)

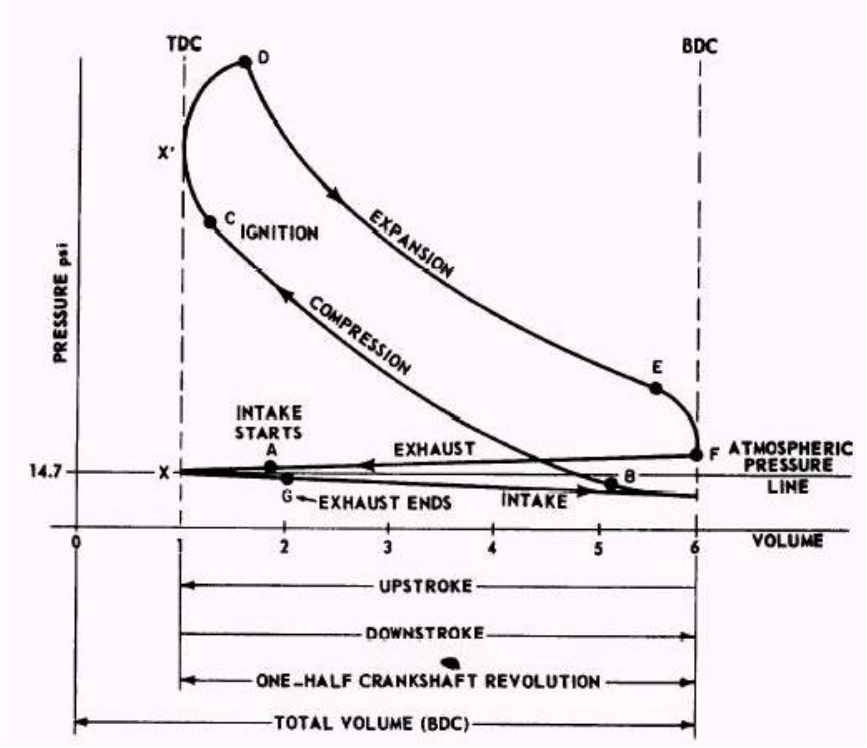

Figure 3: Pressure versus volume (P-V) diagram for a four stroke naturally aspirated petrol engine (Integrated Publishing, 2019)

Figure 3 illustrates pressure versus volume of the combustion chamber through a full four stroke cycle. With reference to the atmospheric pressure line shown on the diagram, it can be seen that the pressure in the combustion chamber is below atmospheric for the duration of the intake stroke, it is this pressure differential across the intake valves that results in the intake charge flowing into the cylinder. Following this, the compression stroke results in decreasing volume and increasing pressure, with the ignition event causing a drastic pressure increase over a minimal change in volume. The expansion (also known as power) stroke then occurs, where work is done on the piston to produce a power output. Finally, the exhaust stroke occurs, with the pressure remaining above atmospheric as the moving piston pushes the exhaust gases out of the chamber.

The power output of an engine can be found from the area under the P-V diagram, that is, the work done on the piston during the expansion stroke, minus the work done by the piston during the compression, exhaust and intake strokes. Evidently, to increase the power output of the engine, we must increase the work done on the piston during the expansion stroke, or decrease the work done by the piston during the compression, exhaust and intake strokes. Work done on the compression stroke is a necessity to compress the air/fuel mixture and to produce power and is primarily a result of volumetric efficiency and compression ratio. Work output during the expansion stroke is a result of the release of energy from the air and fuel mixture and is dependent on a wide range of engine parameters such as lambda, ignition timing, engine geometry etc. Work done during the intake and exhaust strokes is a function of pressure differential over the exhaust and intake valves.

2.2 Increasing Power

When the combustion chamber is treated as a simple, closed system an energy balance can be conducted. That is, $Q_{in} = Q_{out} + W_{out}$ where work is the power output of the engine. Energy in is increased through increasing the amount of fuel brought into the cylinder, however, fuel can only burn and do so effectively if there is the correct amount of air present. Therefore, to increase the fuel mass flow, we must increase the air mass flow also.

Power output can therefore be attributed to a few main parameters; cylinder volume, volumetric efficiency, air/fuel ratio and flow rate, engine speed, fuel type and ignition timing. Some of these parameters are easily tuned within the MoTeC M150, others are geometrically constrained in some way. Geometric constraints are highly resource intensive and expensive to make, often result in reduced reliability. They can also be restricted by the rules of the competition, for example, engine displacement is limited to 710cc (Society of Automotive Engineers, 2019). Increasing engine speed past its designed maximum speed can be dangerous, as the speed is limited by material properties and lubrication. A problem that can occur when increasing engine speed if the valve springs are not stiff enough is valve float (Smith, 2018), where poppet valves may not correctly follow the closure profile of the cam lobe, due to the valve spring used not keeping the valve in contact with the cam lobe. This results in premature valvetrain wear, decreased efficiency and decreased performance. With regards to fuel type used, Formula SAE only allows two fuel types, 98RON and E85.

Volumetric efficiency is considered the most important element when optimising an engine's performance (Ceviz, 2007). Volumetric efficiency is defined as the ratio between the air mass flowing into the cylinder from the intake manifold and the mass of air theoretically inside the cylinder at the intake manifold pressure (Pogorevc & Kegl, 2006), effectively describing the ability of an engine to fill its cylinder.

$$\eta_{Vol} = \frac{2\dot{m}_a}{\rho V_d n} \qquad \textit{Equation 1}$$

Adding more fuel/air mixture to the combustion cylinder results in more energy being released during the combustion event, which exerts a greater force on the piston and hence results in a higher power output. A volumetric efficiency of 100% therefore representative of an engine that can completely fill its cylinder with air, as if it were open to atmosphere. However, due to the pressure losses present in an intake system, most naturally aspirated engines have a volumetric efficiency of approximately 80 to 90 percent (Heywood, 1988). Volumetric efficiency is affected by a wide range of variables, including intake geometry, inlet temperature and pressure, air/fuel ratio, cam profiles, valve geometry, compression ratio and engine speed (Pogorevc & Kegl, 2006).

2.3 FSAE Intake Fundamentals

Within the scope of Formula SAE, where an intake system must always be designed and manufactured to accommodate the rules-mandated restrictor, the intake system is the most effective way to increase volumetric efficiency by minimising the negative effects of the restrictor.

As discussed in the introduction, an intake system in Formula SAE will consist primarily of a throttle body, restrictor, diffuser, plenum and the runner(s), in that order.

The intention of the restrictor is to create a large frictional loss across the reduced cross-sectional area, lowering intake air pressure and therefore air mass available for combustion. According to Heywood's text 'Internal Combustion Engine Fundamentals': *"During the intake stroke, due to friction in each part of the intake system, the pressure in the cylinder p, is less than the atmospheric pressure p_{atm} , by an amount dependent on the square of the speed. This total pressure drop is the sum of the pressure loss in each component of the intake system: air filter, throttle, manifold, inlet port, and inlet valve. Each loss is a few percent, with the port and valve contributing the largest drop. As a result, the pressure in the cylinder during the period in the intake process when the piston is moving at close to its maximum speed can be 10 to 20 percent lower than atmospheric. For each component in the intake (and the exhaust) system, Bernoulli's equation gives:*

$$\Delta P = \zeta_j \rho v_j^2$$

where ζ is the resistance coefficient for that component which depends on its geometric details and v_j is the local velocity. Assuming the flow is quasi-steady, v_j is related to the mean piston speed S_p by:

$$v_j A_j = S_p A_p$$

where A_j ad A_p are the component minimum flow area and the piston area respectively. Hence the total quasi-steady pressure loss due to friction is:

$$P_{atm} - P_c = \Sigma \Delta P_j = \Sigma \zeta_j \rho v_j^2 = \rho S_p \Sigma \zeta_j (\frac{A_p}{A_j})^2$$

This equation indicates the importance of large component flow areas for reducing frictional losses, and the dependence of these losses on engine speed." (Heywood, 1988)

However, as a purpose-built air restrictor is more specific to racing applications, it is not included in this passage. While in this text, Heywood identifies the port and valves as the largest pressure drop, in Formula SAE, the pressure drop through the restrictor is intended to be of great significance also. Therefore, with the implementation of a restrictor mandated by rules, the design of the intake system and the ability to reduce the overall pressure loss in the system is of great importance to improving vehicle performance.

There are several intake design considerations that must be made in order to limit pressure losses in the system and maximise the volumetric efficiency of the engine. The first of these is the basic geometric constraints of runner length and plenum volume, which are highly influential on system performance. Results from previous dynamometer testing using the KTM 690 Duke R are shown below in Figure 4.

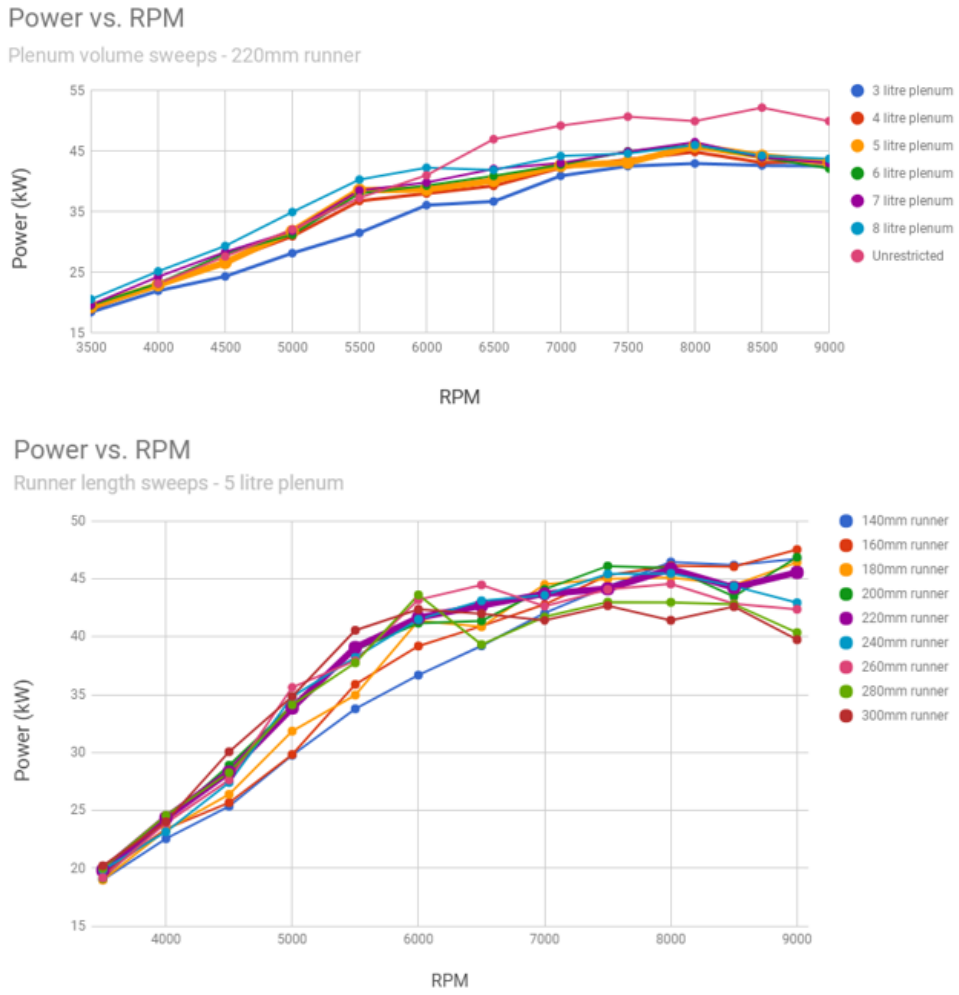

Figure 4: Power vs RPM for a variety of runner lengths and plenum volumes

Plenum volume tuning, particularly of larger volumes, is something that is relatively unique to restricted applications and hence there is considerably less literature available for reference than with other parameters. The plenum volume serves to act as 'air storage' that the engine can draw from during the intake stroke, and then refill as the engine goes through the rest of the four-stroke cycle. The plenum therefore effectively acts to damp the high frequency pressure oscillations of the engine and keep positive flow through the restrictor. Because of this, a larger plenum volume will negate the effect of the restrictor more than a smaller plenum volume, which is apparent through the increased power of larger plenum volumes in Figure 4. The issue with larger plenum volumes is that the pressure in the intake manifold will take longer to change with respect to changes in throttle position, resulting in a delayed throttle response and negatively affecting drivability. This is something that has not been quantified by MMS yet, as the dynamometer only allows for steady state operating, and hence plenum volume must be selected based on a combination of dynamometer testing, Ricardo simulation and driver feedback.

Running length tuning is another geometric parameter used to control the power output of the engine, by taking advantage of the resonance effects present within the intake. The total runner length is defined as the distance from the intake valves to the plenum (Heywood, 1988), or the length of the flow channel from the plenum to the combustion chamber. When the intake valves

open and close, they create pressure waves that travel up and down the runner, reflecting from the plenum as in a similar manner to Helmholtz resonator. When the intake valve opens and the low pressure of the combustion chamber is exposed to the higher manifold pressure, a low-pressure wave travels up the runner and is reflected at the plenum as a high-pressure wave back down the runner, towards the intake valves. If this high-pressure wave reaches the intake valves just before they close, it can produces a 'positive tuning effect' (Heywood, 1988), which can be thought of as 'natural supercharging', increasing the volumetric efficiency of the engine beyond that which it would normally be capable of. Just as this resonance within the intake can have positive effects on power output at some engine speeds, at other engine speeds the effect can be destructive and result in a reduction in power. Therefore, runner length tuning is often done based on deciding the shape of the power curve, with longer runners providing torque peaks at lower engine speeds, and the inverse being true for shorter runners. This is illustrated above in Figure 4.

Finally, the runner is typically joined to the plenum by a bellmouth, which serves to increase air mass flow rate into the runner by reducing pressure loss and increasing the discharge coefficient. The reasoning for this is best illustrated below in Figure 5, that shows velocity profiles through three different ducts. The effectiveness of the flow regime at the boundary at the end of a pipe is considered numerically, as a 'discharge coefficient' (Blair & Cahoon., 2016), which is related to the pressure drop of the fluid as shown in Equation 2.

$$C_d = \frac{\dot{m}}{A\sqrt{2\rho\Delta P}} \qquad \textit{Equation 2}$$

The straight-cut pipe shows the most flow separation, highest pressure drop and hence lowest discharge coefficient. The addition of a simple radius to the end of the pipe greatly reduces separation, and a 'bellmouth' profile shown on the far right eliminates it. Research has shown that when determining the exact profile for a bellmouth, an elliptically profiled bellmouth will outperform an aerofoil profile or simple radius (Blair & Cahoon, 2016). Therefore, in a racing application such as FSAE, where maximum performance is always the goal, the use of an elliptically profiled bellmouth is the superior runner entrance for maximising engine performance.

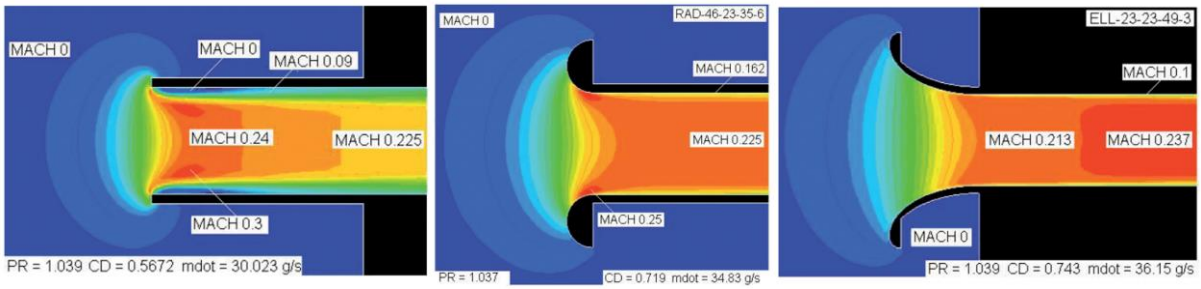

Figure 5: Velocity profiles into different pipe ends (Blair & Cahoon, 2016)

By rules, a 19mm or 20mm restrictor must be used in the intake system after the throttle body, which all airflow to the engine passes through (Society of Automotive Engineers, 2019), in order to limit the power output of the engine. FSAE restrictor design is something that has been researched multiple times by many teams. The general consensus made by this research is that a venturi-style restrictor will offer less pressure loss than an orifice plate, and a smoother restrictor design that avoids flow separation will assist in further minimising pressure loss. This conclusion is intuitive from a basic knowledge of fluid dynamics. The air travels through the restrictor at high velocity and low

pressure, and hence effectively recovering this pressure prior to the plenum is essential for an efficient intake system. This is achieved through the use of a 'diffuser' after the restrictor. As with the restrictor, a large magnitude of research has been undertaken into diffuser design, and when determining the optimum diffusance angle, an angle of 7 degrees will result in the lowest pressure loss, while being the largest attainable angle while avoiding flow separation (Claywell & Horkheimer, 2006).

2.4 Fuel Injection

The KTM 690 Duke R uses port fuel injection, as have all combustion powertrain packages used by MMS since 2011. Port fuel injection offers a much higher degree of tuneability than a carburettor as it is all controlled by the ECU, which allows for easier starting and greater efficiency.

It is well-established fact moving the injector further away from the inlet port can assist with improving the air fuel mixture quality when a large injector is used at high fuel and air flow rates, as larger fuel injectors tend to have poorer vaporisation characteristics. However, this comes at the expense of a much greater difficulty idling and maintaining drivability at lower engine speed and manifold pressure sites. Dual stage injection systems mitigate this issue by using a smaller flowrate injector close to the inlet valve for lower load sites, and a higher flowrate injector for higher load sites. This was tested by MMS in 2018 but due to the relatively short runner length used on the car, the injectors remained quite close together and the effects compared to using a single injector were negligible.

Therefore, the previous research conducted by MMS on the KTM 690 Duke R had determined that the ideal injector position is on the runner, pointing directly onto the back of the intake ports, and hence this will be used to model the injector boss positioning in CAD. The testing also confirmed that the highest-performing injector was a Bosch 347cc/min injector operating at 5 bar differential fuel pressure, and hence will be used for M19-C.

2.5 FSAE Rules

The rules that apply to the intake system are comprehensive and large in number, with the entire 2019 FSAE and 2019 Formula Student rulesets being included in Appendix A. The intake system must meet all of these rules requirements in order to pass scrutineering, and for M19-C to compete at competition. Of particular interest is the aforementioned 20mm circular restrictor required in the intake system to limit power output of the engine, as well as the rules concerning the packaging of the intake system. These rules specify that the intake system must lie within the 'surface envelope' of the vehicle, as shown in Figure 6. This greatly constrains the geometrical freedom of the system and has a large influence on the attainable size and shape of the final part.

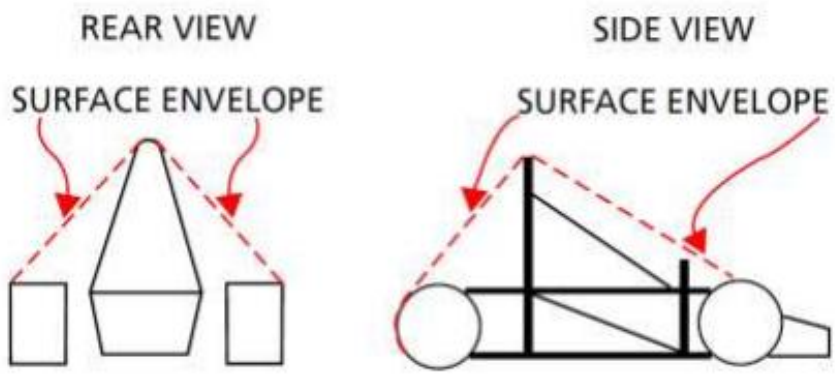

Figure 6: Definition of surface envelope of an FSAE vehicle (Society of Automotive Engineers, 2019)

2.6 Other Teams

While the transition to a 3D printed intake and ETC is a first for Monash Motorsport in 2019, there are other teams that have been doing one or both of these already. Within Australia, multiple teams were contacted for discussion regarding design and implementation of both systems. It is worth noting that the teams contacted both used Yamaha WR450F engines in 2018, which are of considerably smaller displacement and utilise a 'reversed head' design, with the intake ports at the front of the engine and the exhaust ports at the rear. Hence, geometrical parameters and packaging constraints are vastly different between their vehicles and M19-C.

University of Wollongong Motorsport (UOW Motorsport) were contacted during the design of the intake system, and discussions had with one of their previous intake part designers, who had designed an SLS printed intake system in past. The recommendations by him were to ensure the inherently porous SLS printed material was sealed to prevent ingress of moisture, fuel and dirt, to use structural, linear FEA at absolute vacuum and to keep the geometry convex at all points to assist with strength. He also mentioned that no post-processing of the intake system was required other than the resin coating, as the surface finish of laser-sintered nylon is quite good.

University of Queensland Racing (UQR) also implemented a 3D printed intake system and a Bosch ETB in 2018. They were not contacted for design assistance, but rather advice on the specific scrutineering requirements for the use of ETC at competition. They advised that the same level of detail was involved in their ETC failure modes and effects analysis (FMEA) as that of their electric car. Hence the same amount of time and consideration was allocated to this as MMS' 2019 electric vehicle, M19-E's, FMEA.

3. KTM 690 DUKE R

The 2019 KTM 690 Duke R, originally from the road bike of the same name, is the selected engine for M19-C. KTM single cylinder engines were considered for M19-C due to ongoing financial and technical support from KTM Australia, and the rear of the chassis being narrowed for more aerodynamics packaging space, disallowing any multi-cylinder engines. From there, the decision was based on points simulations conducted within the teams point-mass competition simulator, Webb Sim.

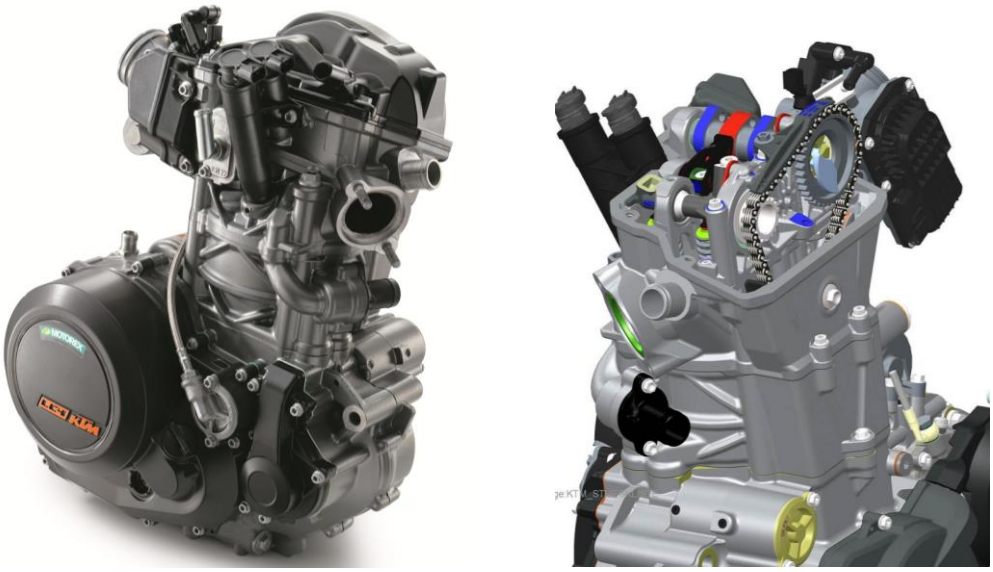

Figure 7: KTM 690 Duke R (Brasfield, 2015)

These simulations showed that the 690 Duke R in turbocharged and naturally aspirated form were the two highest points potential concepts, and that the turbocharged concept would be worth 10 more points than in naturally aspirated form. However, previous turbocharged MMS cars (2013-2016) have failed to capitalise on their increased points potential offered by their concepts. This is attributed to the increased complexity and time involved in designing, manufacturing and calibrating the turbocharged powertrain, and the decreased reliability leading to lost testing time. Missing one important testing session could more than negate any points gains made by the turbocharger.

Hence, the highest points-potential concept remaining was the KTM 690 Duke R in naturally aspirated from. This decided the basic concept of the intake system and allowed data gathered from 2017 and 2018 to be used and built upon for intake design and validation.

4. CONTROL HARDWARE

In another first for Monash Motorsport, a MoTeC M150 ECU (shown in Figure 8) will control the car and log sensor data in 2019. This replaces the previous control and logging setup used from 2011-2018, where a MoTeC M400 ECU and MoTeC Advanced Dash Logger (ADL) were used. This has increased the logging capacity of the car from 8MB to 248MB, greatly increased the number of sensor inputs and allows for multiple CAN buses to be utilised. Custom firmware can also be created and implemented into the ECU, which is critical for implementing the plausibility checks required by rules when using ETC. Finally, the M150 has built in ETC capability and hence is not something the team will need to spend time creating and validating.

Figure 8: MoTeC M150 ECU (Cody Phillips Racing, 2019)

Specific to the intake system, and its design and validation, the M150 controls the fuelling and ignition timing of the engine. To determine the fuelling, the M150 uses manifold pressure (MAP), air temperature and engine speed to determine the duty cycle of the fuel injector, hence secure mounting of the temperature and pressure sensor (T-MAP) sensor and fuel injector are crucial for successful and reliable intake operation.

The table that controls the fuel delivery (known as the Engine Efficiency table) is calibrated by holding the engine at the desired engine speed (RPM) and adjusting the efficiency values until the target lambda value is reached. Lambda is measured using a lambda sensor (sometimes referred to as an oxygen or O2 sensor) that measures the amount of oxygen present in the exhaust gas (AutoMap, 2012) to infer the air/fuel ratio entering the combustion chamber. Previous lambda sweeps on the dynamometer with the KTM 690 Duke R have shown that peak power of the engine occurs at a lambda of 0.84, and peak efficiency at 0.97. Fortunately, with the M150, once the efficiency table is calibrated, fuel tuning is as simple as changing the target lambda table, and the amount of fuel delivered adjusts automatically to match.

5. INTAKE DESIGN

5.1 Requirements

The primary function of the intake system is to deliver a controlled amount of fuel and air to the engine, in order to facilitate combustion within the combustion chamber, in such a way that passes all relevant rules and hence will allow the car to drive at competition.

With regards to rules requirements, this means that the intake must be designed to meet all rules set out in Appendix A, or else the car will be unable to drive at competition. For example, this means that there must be a 20mm circular restrictor after the throttle body, that the intake must be packaged within surface envelope and that the system must mount to both the engine and the chassis, and mounts to the chassis must incorporate vibration isolation to allow for relative movement between the engine, chassis and intake system.

More specifically within the context of M19-C, where high performing parts are both desirable and necessary for the car to be competitive, the intake too must perform as strongly as possible. The best metric for evaluating the intake's performance is, as discussed prior, the volumetric efficiency. The aerodynamic performance of the system must be as strong as possible, in order to minimise the pressure losses through the system and increase volumetric efficiency. This can be achieved through following best engineering practises with regards to the restrictor, runner and diffuser, while avoiding sharp bends and sudden changes in cross-sectional area, geometry known to cause pressure losses in any system that transports fluid.

Another requirement that must be considered is the need to minimise mass. Every component on M19-C adds mass, and mass makes it more difficult to accelerate laterally and longitudinally, therefore the need to minimise mass cannot be ignored. The distribution of this mass on the car influences overall vehicle performance too, as a higher centre of gravity lowers the performance potential of the vehicle. Therefore, the intake should be designed to have the lowest possible centre of gravity attainable.

The intake system, in conjunction with the tuning of the engine, mostly determines the drivability of the car from a powertrain perspective. Having a predictable, reliable and consistent engine response is crucial to driver confidence, which in turn is necessary for the cars to perform to their full potential at competition. It is worth noting here that an underpowered car can still be an extremely drivable one, the two are not dependent. Rather, if the engine is calibrated correctly, a large proportion of the drivability comes from the throttle, with a throttle that is too large, or a throttle profile that is too aggressive not having the required resolution to effectively modulate airflow to the engine.

5.2 Throttle Selection

One of the first aspects of the intake system that must be considered is the throttle body. As discussed prior, the throttle has a large part to play in the drivability of the car, which in turn is crucial to drivers being able to extract the full potential from the car, whatever that may be. When choosing a throttle body, it is important to consider several aspects. Firstly, control type is a large choice that must be made, as a throttle body can be manually actuated (usually by means of a cable attached to the throttle pedal) or electronically actuated in a drive-by-wire system, where a sensor

on the throttle pedal relays torque requests to the ECU, which actuates the throttle body accordingly. Secondly, bore size must be considered as this will determine the manifold pressure for a given throttle valve position and engine speed, and be largely influential in determining the drivability of the car. Cost and mass are considered also, as reducing mass and cost are both beneficial to the team. Several throttle concepts are discussed below.

The first throttle body considered is the AT-Power 28mm mechanically actuated throttle, shown below in Figure 9. This throttle body has been used by the team since 2011 on KTM single-cylinder engines, including the KTM 690 Duke R in M17-C and M18-C, and has largely performed without fault. Rules concerning the use of manual throttle bodies are much less comprehensive than ETB's and the only sensor required is one TPS, making it a simple system to implement. It is also intrinsically immune to plausibility failure as a result of its actuation method. This throttle body does however have several drawbacks. The throttle cable and its sheath have proven to cause drivability issues, particularly in events such as skid pad where steady-state throttle and fine adjustments are crucial. This is due to the sheath wearing and creating stiction with the throttle cable. The driver then must input a significant amount of force to the pedal to overcome this stiction which often results in the driver overshooting the desired throttle position and torque request. The car must also be tuned to idle at the same throttle position that it is able to start at, which means that in order to achieve a low MAP at idle to reduce noise output, the car will be quite difficult to start. Finally, cable adjustment at the pedal box and throttle body must be undertaken every time the throttle pedal is worked on or the throttle cable is replaced, which is a difficult task and can take two people up to an hour to complete. The estimated throttle system mass for this solution was 700g, at a cost of approximately $800.

Figure 9: AT-Power 28mm Throttle Body (left), Bosch 32mm Electronic Throttle Body (right), (AT Power, 2019), (Bosch, 2019)

The second throttle body considered is the Bosch 32mm Electronic Throttle Body, shown on the right of Figure 10. This bore size is the smallest size ETB commercially available, and being larger than the 28mm manual throttle body, will not choke the engine but may provide less resolution. ETC has not been used by MMS in the past, and rules concerning the use of ETC are much stricter than with a mechanical system. There are also plausibility checks that must be implemented into the M150 ECU firmware which shut down the ETC if an error occurs. A Brake System Plausibility Device (BSPD) must also be designed and implemented to determine if hard braking and a throttle position of greater than 10% are occurring simultaneously and open the shutdown circuit of the car if this is true (Society of Automotive Engineers, 2019). However, as this rule is being implemented for mechanical throttle control in the Formula Student Ruleset (governing the European competitions) from 2019 onwards, it is only a disadvantage for the Australian competitions.

A multitude of advantages exist from using ETC also. Starting in all conditions, particularly in cold temperatures, is much easier as the throttle can be automatically controlled by the ECU during the start-up process. Idle can also be set to a lower value, to decrease noise levels. Custom throttle profiles can be implemented for different drivers and events, providing particularly large advantages in events such as skid pan, where 0.1s is worth 7.7 competition points (Formula Student, 2018). The throttle can also be automatically controlled during shift events, which will make downshifts in particular a lot smoother, reducing the amount that the car is unsettled and eventually allowing for the removal of the pneumatic clutch, a mass saving of 800g. Throttle-based launch control can also be implemented to maximise the longitudinal acceleration of the car, keeping the slip ratio of the rear wheels closer to the target slip ratio when accelerating than traditional methods such as ignition cutting. A 0.1s decrease in time in the acceleration event correlates to 5.3 competition points (Formula Student, 2018). The Bosch ETB also incorporates two throttle positions sensors (TPS's), make the throttle itself rules compliant with no modification. The estimated throttle mass for this solution was 1050g at a cost of $650.

Therfore, as a result of its lower price, increased serviceability and tunability, and potential for increasing the concept utilisation of the car, the Bosch 32mm Electronic Throttle Body was selected as the throttle body for M19-C.

5.3 Engine Simulation

Throughout the design process, Ricardo 1D engine simulation was used to assist with guiding correct design decisions and quantifying major concept changes, such as plenum volume and runner length. Originally, it was planned to be used to greater effect in correlation with CFD results, which were intended to allow for the extraction of discharge coefficients of sections of the intake system, that could then be input into Ricardo to quantify the performance change between iterations. However, due to reasons discussed later in this report, the CFD was not able to be utilised in this way.

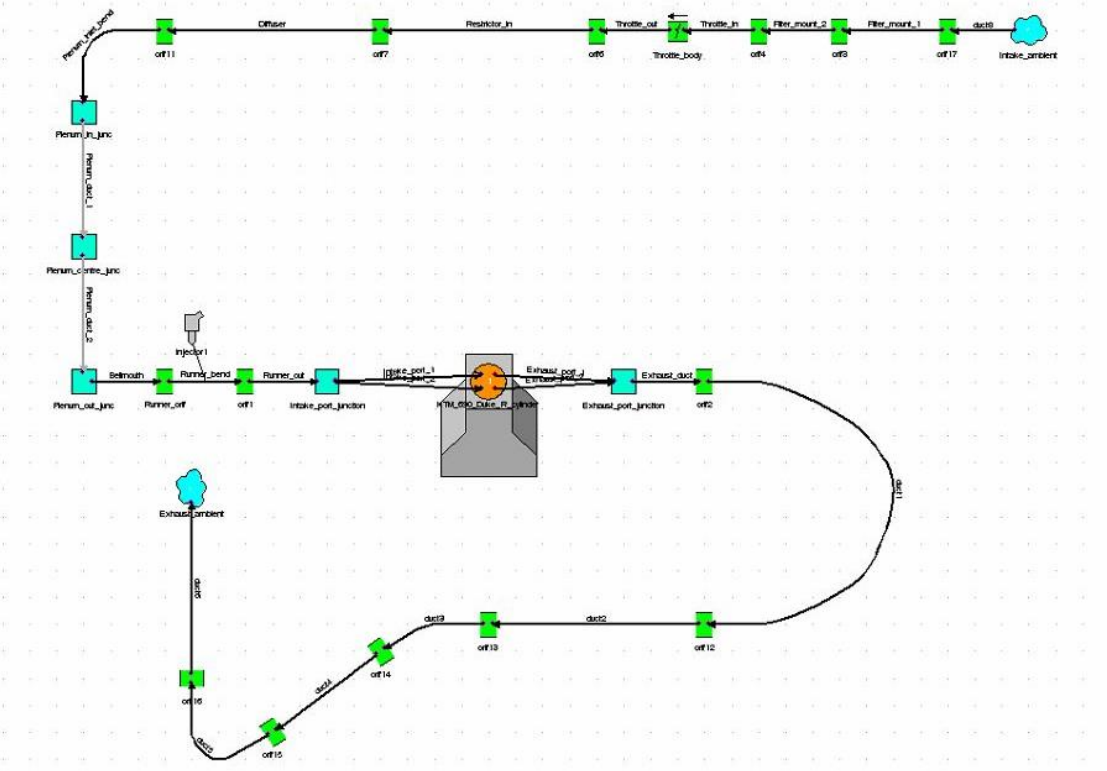

Figure 10: Ricardo 1D engine simulation setup

The model of the KTM 690 Duke R within Ricardo was built and calibrated by a previous MMS team member, William Jenkin. The model was calibrated against dynamometer data and sweeps of different parameters such as plenum volume and runner length to confirm it to be not only accurate to the intake system on the dynamometer, but to accurately model trends and performance differences when major parameters are changed. A screenshot of the model set-up in Ricardo is shown in Figure 10.

5.4 Parameter Selection

Before any intake system concepts could be produced, it was first important to select the basic geometrical parameters. This would then largely determine the viability of different packaging concepts before significant time was invested in them, streamlining the design process.

The two key factors that would influence concept generation are the runner length and plenum volume. A combination of previous dynamometer data and Ricardo engine simulation was analysed in order to determine the parameter values that would result in maximum power being extracted from the engine, while staying within realistic boundaries. For example, Figure 11 shows that increasing plenum volume (on the dynamometer) on the KTM 690 Duke R does continue to offer increased performance from a power perspective up to at least 8 litres, but the logistics of packaging a plenum of that size immediately rule it out, without considering the potential adverse effect on throttle response and increased mass.

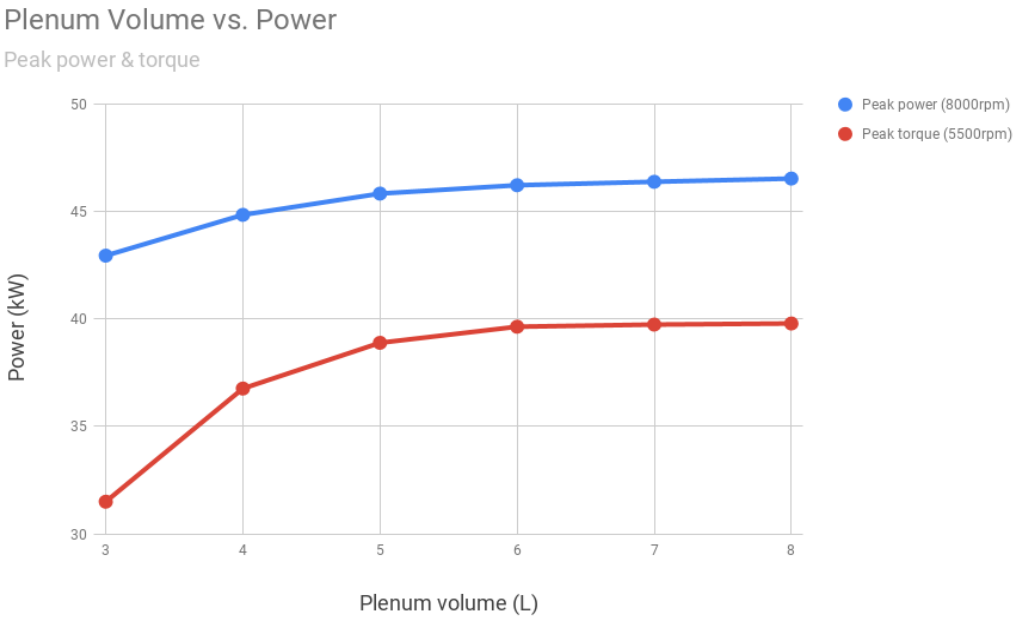

Figure 12: Plenum volume vs power at peak power and peak torque sites

Through further analysis of Figure 11, it can be seen that despite the continual increase in power and torque, returns significantly diminish after 6 litres. As plenum volume increases, so does the mass and difficulty of packaging the system. The drivability can also be adversely affected. With consideration to throttle response and drivability, a plenum volume of 5 litres was utilised on M17-C, which according to driver feedback, did not suffer any adverse effects from its large volume. It was therefore assumed that a 20% increase in plenum volume to 6 litres, the point of diminishing returns, would not significantly adversely affect the drivability of the car. Finally, Ricardo data shown in Figure 12 validates the dynamometer data in Figure 11 and therefore 6 litres was selected as the preliminary plenum size.

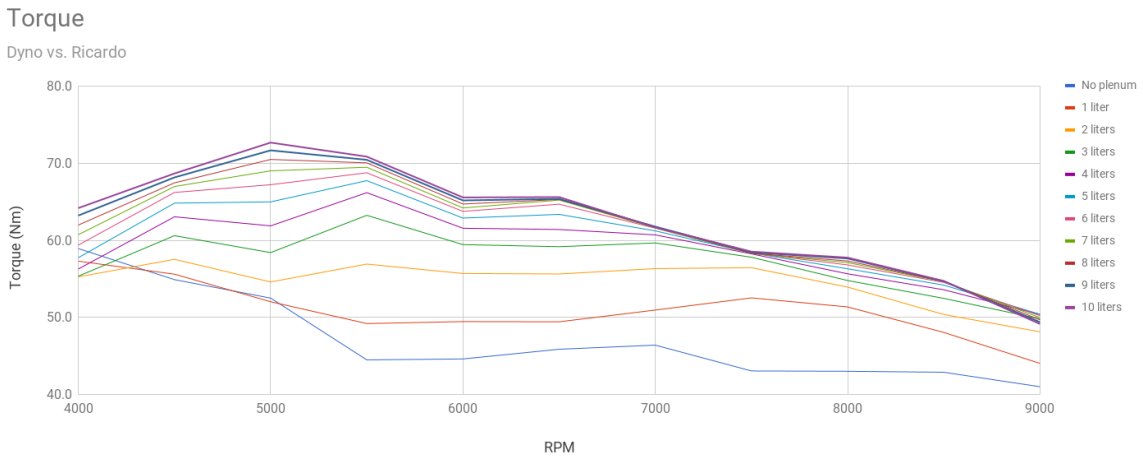

Figure 11: Ricardo torque vs engine speed for a range of plenum volumes

With the approximate size of the plenum decided, its positioning relative to the intake port of the engine is dictated by the runner length. As discussed in the literature review section of this report, runner length tuning in naturally aspirated concepts is particularly important when deciding the shape of the power and torque curves of the engine, as acoustic effects have a considerable influence on volumetric efficiency. A longer runner tends to result in a torque curve shifted towards

lower engine speeds, and a shorter runner results in a torque curve shifted towards higher engine speed. In Figure 13, a histogram of the engine speeds most used by drivers when they are requesting torque (throttle position >80%) during an endurance event is shown and shows that having a broad torque curve from 6000-9000 rpm is most desirable, as this is where power is needed from the engine most of the time.

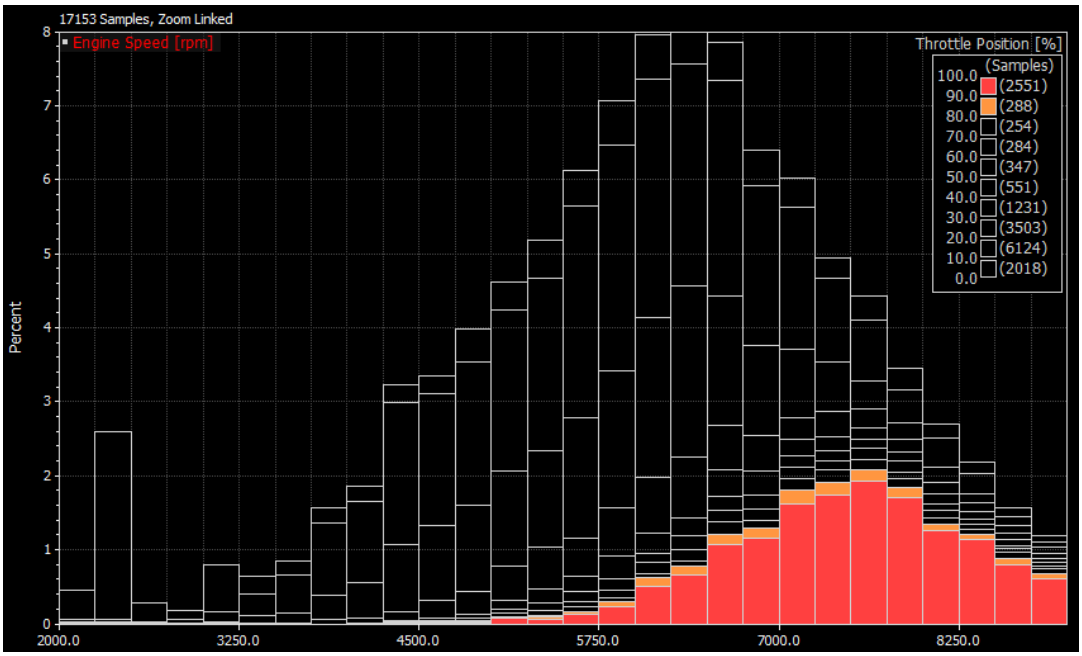

Figure 13: RPM histogram for an endurance event

Dynamometer data and Ricardo data, showing the torque curves of different runner lengths, is shown in Figure 14. Analysing these with respect to the target engine speed discussed above led to the selection of a preliminary runner length of 220mm. This allows for a broad, flat torque curve to be achieved, and ensures that packaging of the runner is possible without large or sharp bends. In combination with the 6-litre plenum volume, it ensures that packaging of the concept is realistically possible, particularly with the geometrical freedom offered by the SLS printing technique.

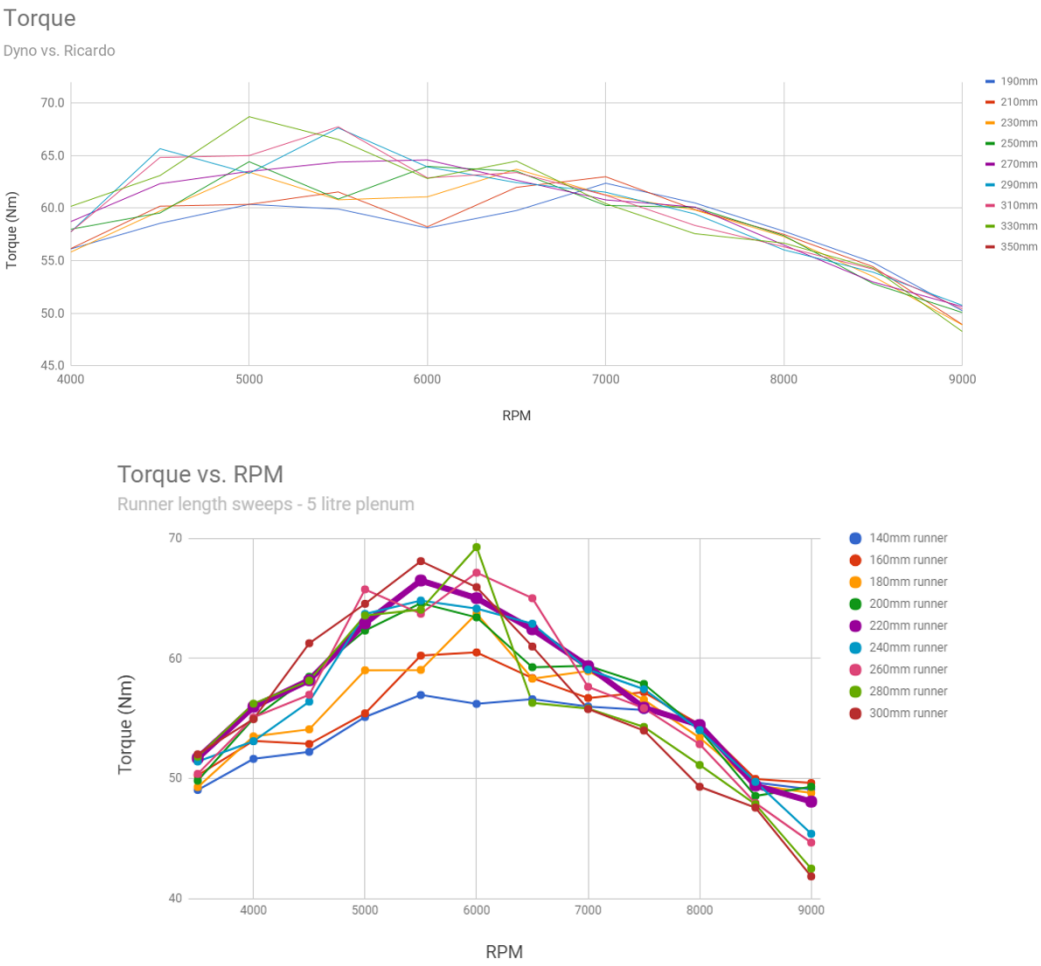

Figure 14: Ricardo and dynamometer torque vs. engine speed curves for a range of runner lengths

5.5 Manufacturing Technique Selection

For Monash Motorsport to justify the utilisation of 3D printing for the manufacture of the intake system, it was important to justify why it should be used compared to conventional methods, and if selected, which 3D printing method should be used.

The primary advantages of selecting 3D printing are a reduced manufacturing time and a greater freedom of geometry when compared to traditional methods. Having almost limitless geometry in turn, allows for the creation of geometry that reduces pressure losses through the system guided using CFD analysis and 1D simulation. This will allow for a system that results in a higher volumetric efficiency, giving increased power and efficiency. It also enables the production of a system which meets stress and deflection goals for the least mass possible by using FEA to guide structural design, increasing the performance of the car by decreasing mass. It is also estimated that compared to a more conventional fabricated intake, 25-man hours of manufacturing are saved. These are then man-hours that can be spent on further designs and improvements to the system, or on further testing and calibration once it is received. Another advantage, that is more specific to MMS, is that 3D Systems are a Platinum-level sponsor of ours and offer a range of printing and post-processing services free of charge. This means that the high price of 3D printing a large object such as the intake system is negated. The freedom of geometry attainable with 3D printing is also possible to achieve

with a composite intake, but the tooling cost, material cost and 45 additional hours of manufacturing time make the method financially and practically unviable.

Although there are many advantages to 3D printing the intake system, there are disadvantages that must be considered also. Because of the geometrical freedom offered by the method, a far greater amount of time must be spent on the design of the system to utilise it well. This requires learning and utilising complex surfacing techniques in CAD, ensuring that the CAD is perfect and mates up with everything perfectly, because the system cannot be test fitted and checked during the manufacturing process in the same way that a conventionally fabricated system could be. FEA simulations must be setup and run to guide the structure of the system, to ensure that the mass is kept to a minimum, and CFD analysis should also be used to guide the internal geometry of the system. All of these result in a much more complex and demanding design process than a traditional system. The repairability of the system is decreased too, as a major failure cannot have a solution quickly manufactured using simple hand tools and a welder.

Overall, the advantages of the 3D printing method outweigh the disadvantages, with the potential performance increase and reduced manufacturing time seen to be worthy of the increased complexity of design and decreased repairability. With 3D printing as the chosen method, the 3D printing technique must also be decided on. Many types of 3D printing are available, each with their own advantages and disadvantages. Viable options considered for the manufacture of the intake were Fused Deposition Modelling (FDM), Stereolithography (SLA), Selective Laser Sintering (SLS) and MultiJet Fusion (MJF). FDM printing uses the extrusion of a melted filament to build a part, with the printhead' and extrusion nozzle moving in the X and Y direction, and the print bed moving in Z. SLA printing utilises a resin bath, which is cured layer-by-layer using UV light. SLS and MJF both utilise a 'powder bed' in which the raw material is kept. SLS printing sinters the material together using a laser, while MJF deposits detailing and fusing agents onto the powder, that are then heated and sintered using UV light.

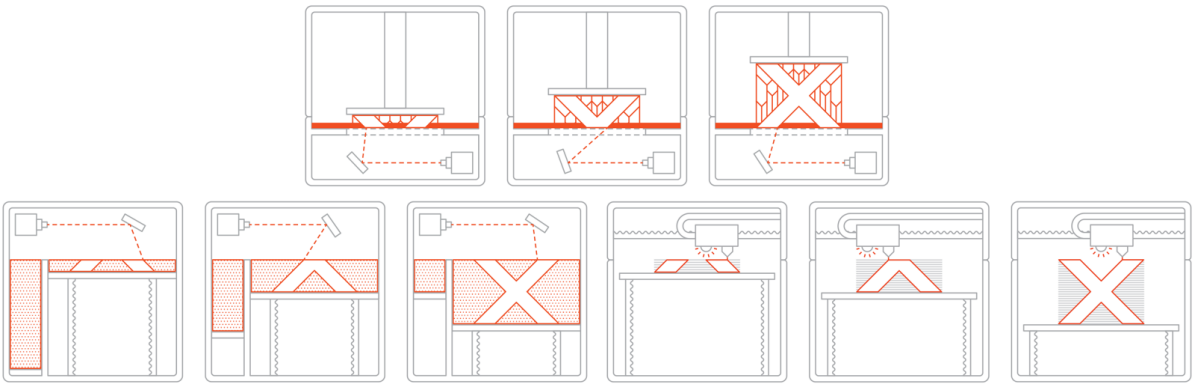

Figure 15: Graphic representation of: SLA (top), SLS (left) and FDM (right) (All3DP, 2018)

One undesirable trait of 3D printed materials is that almost all of them have some level of anisotropy. This is due to the way that they are manufactured, which is one layer at a time and results in less effective bonding between print layers than within them. Hence, the mechanical properties, such as tensile strength, Young's Modulus and elongation at break of the printed product are often worse in the print (Z) direction than in the print plane (X&Y). FDM printed materials are affected most heavily by this, and hence are generally not recommended to be used in structural applications. SLS and SLA also display some anisotropic properties, but to a lesser degree. These

must be compensated for in some way during the structural analysis of the system, to ensure that its strength is not over-estimated. A more isotropic material is hence ideal for the intake system, where stresses are applied in all directions and print orientation is assumed to be unknown.

Another consideration is the way that the part is printed when the geometry involves overhangs. Methods that create free-standing parts, such as FDM and SLA, require support structure to be printed to support the part during the printing process. This structure then must be removed after the print and is often time consuming and difficult. Methods that utilise a powder bed, such as SLS and MJF, do not require a support structure because the un-sintered powder provides support for the part and is simply blown out of the finished product. Due to the intake system comprising of very large and enclosed volumes, printing without support structure will reduce post processing time and increase surface quality. SLA printed parts, as well as requiring support structure, tend to be quite brittle and are also not recommended for structural applications.

This then meant that the two printing methods to choose between were MJF and SLS printing. Parts printed using MJF tend to be completely isotropic in nature, while printing out of the same materials offered by SLS. Hence, MJF would be the ideal printing method but unfortunately is not offered by 3D Systems Australia. Therefore, due to its mechanical properties and availability, SLS is the chosen printing and manufacturing method for the intake system.

5.6 Concepts

With manufacturing technique, throttle body and basic geometric parameters chosen, the final major concept decision was the packaging choice of the system. Due to the 6L plenum size and 220mm runner length combined with the tighter packaging constraints of M19-C's chassis, packaging the intake within the 'surface envelope' would prove a difficult task, and narrowed the choice down to two general concepts.

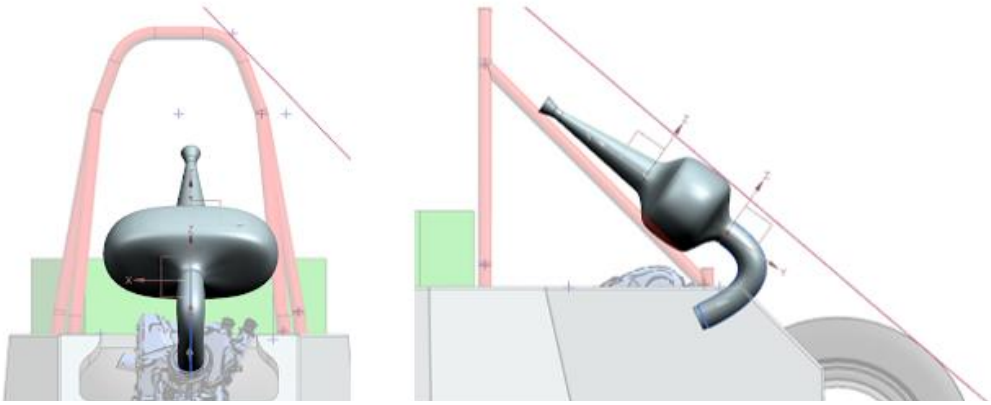

Figure 16: 'Top-mounted' intake system concept

The first of these concepts, shown in Figure 16, is a 'top mounted' concept. This concept was initially promising for the symmetry that it offers and straight flow path for the air from the throttle to the plenum. However, to package a runner of the required length, a sharp bend would be required to turn the air approximately 90 degrees into the intake port and the pressure drop through here would be considerable. Another consideration would be the difficulty of mounting, as the intake and the 800g ETB would likely need to be mounted to the roll hoop by some types of brackets which

would prove difficult to manufacture accurately. This concept also has an extremely high centre of gravity (COG) and carries with it a points penalty of -1.29 considering only the change in height of the ETB compared to the side-mounted concept. 1kg of mass added to the car is a points penalty of approximately -1 point, and hence this concept can be eliminated due to its increased COG and difficulty of mounting.

The remaining option was then a 'side-mounted' concept, shown at the concept level of development in Figure 17. This design has a lower COG and is therefore immediately worth 1.29 points more than the top-mounted concept. The asymmetry of the concept is unlikely to be an issue, as other asymmetry inherently exists on the car, such as the exhaust manifold. The side mounted concept suffers from the air needing to turn through almost 180 degrees from entry into the air filter to the intake ports, but the organic geometry offered by SLS printing should mostly negate this. The mounting of the system should be much simpler also, with all mounts able to go directly to the monocoque. This was therefore the chosen packaging concept for the intake system of M19-C.

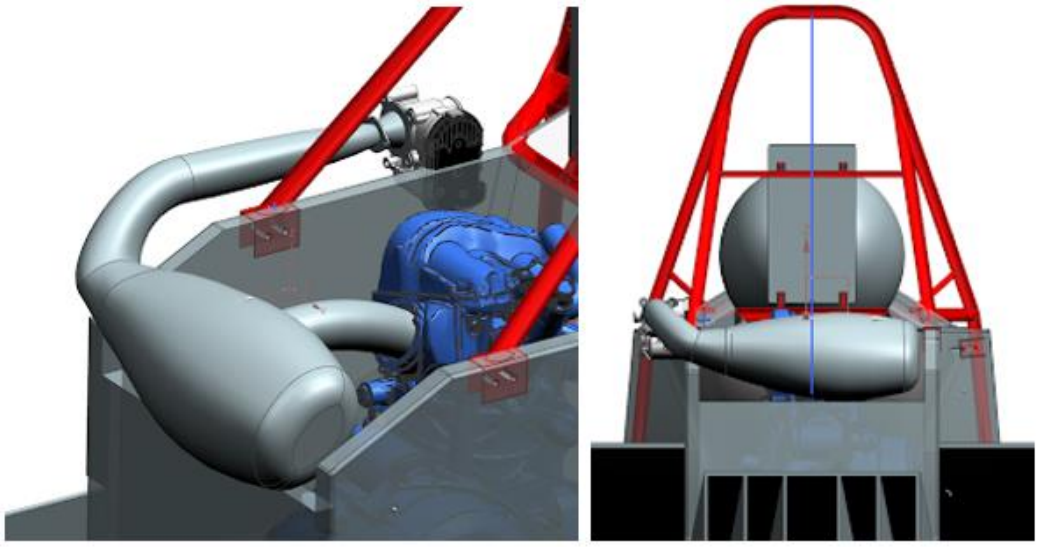

Figure 17: 'Side-mounted' intake system concept

5.7 Material Selection and Physical Testing

With SLS printing as the chosen method, the next consideration must be for material type. Due to the requirements of the intake system including interfacing with the engine and delivering the air/fuel mixture to the combustion chamber, the material must have a high temperature resistance and must be chemically stable in 98RON and E85 fuels. The material must also have a high specific stiffness and specific strength, to assist with keeping the part as light as possible. 3D Systems Australia and US were contacted for technical advice and recommended three variants of Nylon-12, the most common SLS printing material. These were DuraForm GF (Nylon-12 with glass beads), DuraForm FR (UL-94 rated Nylon-12) and DuraForm HST (Nylon-12 with composite fibres). These are compared in the table below:

Material	DuraForm GF	DuraForm FR 1200	DuraForm HST
Description	Nylon 12 w/ 30% glass beads	Fire-resistant Nylon 12	Fibre-reinforced Nylon 12
Density (g/cm3)	1.49	1.02	1.20
Yield Strength (MPa)	27	n/a	n/a
Ultimate Tensile Strength (MPa)	26	41	48
Tensile Modulus (GPa)	4.07	2.04	5.48
Ultimate Flexural Strength (MPa)	37	62	83
Flexural Modulus (GPa)	3.11	1.77	4.4
Elongation at break (%)	1.4	5.9	4.5
Qualitative Surface Finish	Good	Great	Average

Table 1: Nylon-12 Properties, as supplied by 3D Systems (3D Systems, 2019)

From the above options, DuraForm FR and HST appeared to be the best two options, with HST having the highest strength and FR having the lowest density. 3D Systems Australia have also successfully printed brake booster reservoirs using DuraForm FR (brake fluid is highly corrosive), showcasing its chemical stability. Inversely, 3D Systems US stated that the chemical stability of DuraForm HST is quite poor and needs to be sealed. This in itself is not a problem, but if any damage were to occur to the part and sealing method compromised, the entire part would begin to degrade. This eliminates the DuraForm HST from a reliability perspective. The DuraForm FR has half the stiffness of the DuraForm GF and hence while easily passing stress requirements, will deflect by double the amount of the DuraForm GF for the same part and loading. It therefore requires considerably more material than DuraForm GF to pass deflection requirements and is ruled out due to its lack of stiffness. Therefore, DuraForm GF was selected.

The surface roughness of SLS printed parts is considerably higher than that of aluminium or carbon fibre. The surface finish of the DuraForm GF is also unable to be significantly improved through sanding, as the inherently porous nature of the material as well as the glass beads prevents the surface from becoming smooth. Research has shown that the surface roughness of glass-bead filled Nylon-12 is approximately 40µm (Negi et al., 2014) compared to a surface roughness of

approximately 5µm for aluminium. The difference in power output is approximately -0.15kW of peak power, as simulated in Ricardo with the results for a range of surface roughnesses shown in Figure 18. While this is relatively insignificant (0.3% reduction in peak power), in a racing application where every bit of performance counts, it was decided that investigation into improving the surface quality of the material should be pursued.

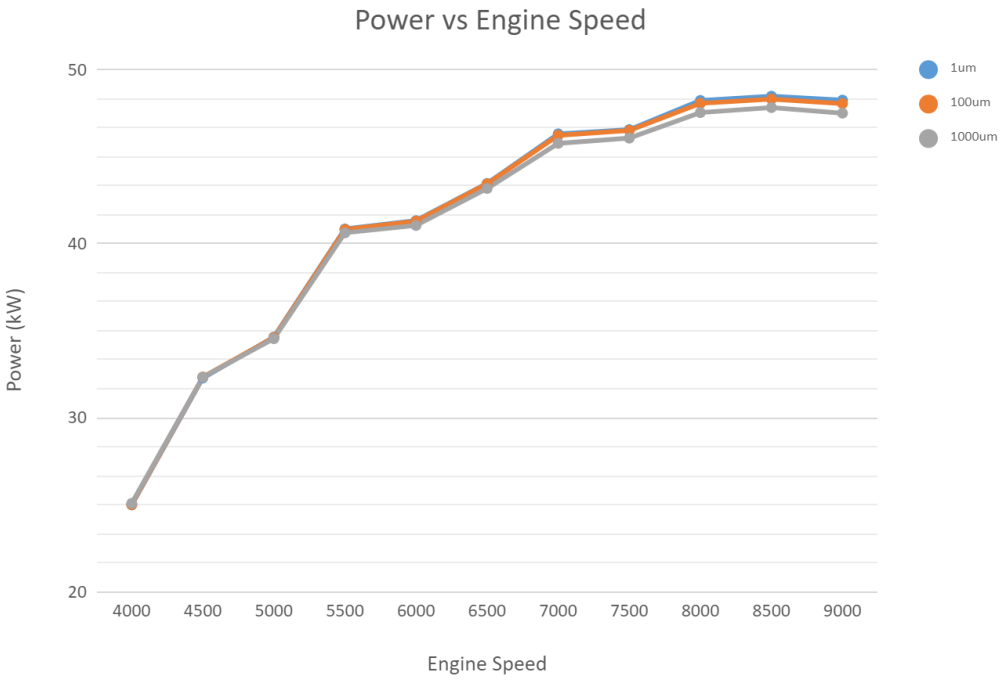

Figure 18: Power vs engine speed for a range of surface roughnesses

Following the selection of the material to be used, several parts were ordered from 3D Systems to determine the intricacies of the system and the post-processing that should be conducted upon receiving it from 3D Systems. These test pieces included a manifold pressure barb (required for the fuel pressure regulator) to determine whether printing one onto the intake would be too fragile to withstand the often rough treatment parts on the vehicle receive. It was found that breaking the barb was extremely difficult and hence it could be incorporated onto the system. Test pieces for the mounting of the T-MAP sensor were also printed, as this could determine the viability of captive nuts in the system and the accuracy of printing O-ring bores into the system. It was found that the accuracy of the printing method was accurate enough for printed O-ring bores to work as expected with no post-machining required, confirming the viability of printing the T-MAP sensor mount and injector boss straight onto the intake system, with details of the T-MAP mounting solution shown in Figure 19. This was beneficial as it reduced the amount of manufacturing required from the team and improves the aesthetics of the part

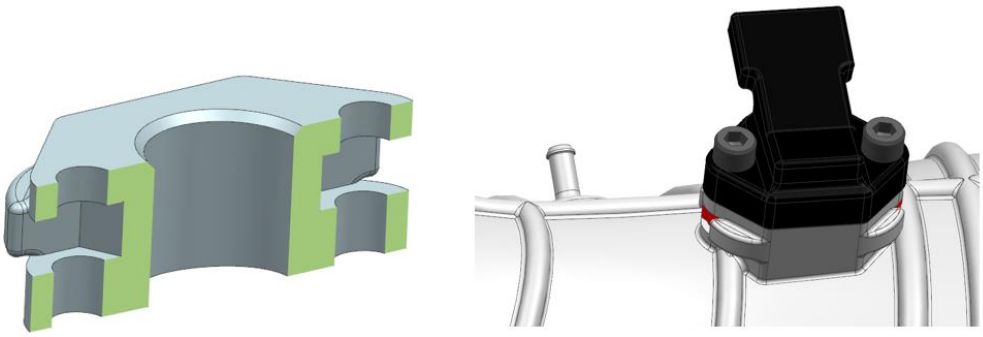

Figure 19: Cutaway view and implementation of T-MAP sensor boss

Finally, sealing and surface roughness improvement testing was carried out. To do this, small bowls were printed and fuel placed into them overnight. As can be seen in a photo taken shortly after the fuel was poured in (Figure 20), the porous material instantaneously soaks up the fuel, where it can be seen 'climbing' the side of the bowl. This evidently posed a safety hazard, as a fuel-soaked intake would cause a significant fire risk. In order to attempt to mitigate this, the inside of the bowl was coated with a thin layer of epoxy resin (AMPREG 22). It was found that sealing the product with an epoxy resin allowed it to become impermeable fuel and furthermore, when lightly sanded the surface finish was much more similar to that of aluminium. 3D Systems were contacted about sealing Duraform GF and said that they could coat it in house in a resin bath, and that they had made brake cylinders using this process before. This was elected as the sealing technique as it minimises post-processing undertaken by MMS. Epoxy resin remained a viable option for improving surface quality on surfaces that required a smoother finish, such as the diffuser and the runner.

Figure 20: Fuel absorption of the unsealed DuraForm GF

5.8 Structural and Flow Simulation

In order to utilise the freedom of geometry uniquely offered by the 3D printing process, it was determined that as well as the 1D simulation, 3D simulation would be utilised as well. The proposed plan was for steady-state CFD to be conducted on the first portion of the intake through to the plenum entrance, as this is where the flow is least transient. This would guide the internal geometry of this portion of the intake system, where the most pressure loss and recovery occurs. FEA would be used to guide appropriate use of material and stiffening structures on the intake system and meet stress and deflection targets while keeping mass to a minimum.

Due to the limited time available in the MMS design period (approximately 2 months), it was decided that a simplified FEA setup would be pursued, allowing more time for iteration and analysis. In hindsight, as discussed later in this section, this was a poor decision as an accurate simulation setup is key to having dependable results. The printed portion of the intake system is mounted through five different points. This includes two bolted connections to the restrictor, two bolted connections to soft mounts to the chassis at the base of the plenum, and rubber booty connecting the intake runner to the inlet port of the engine. In the interest of time constraints, these were all modelled as fixed supports that likely over-simplified the model.

For meshing within ANSYS, a tetrahedral-hexahedral, first and second order mixed mesh was used, as this combination can easily fit more complex geometry with fewer elements, facilitating faster simulations. The mesh was further refined around mounting points and any other areas of interest, with a general mesh sizing of 4mm used. The mathematical errors that can arise from using this type and size of mesh on a large, thin-walled part such as the intake system were not considered at this point but were realised later in the year and further refined.

A custom material had to be created within the ANSYS software before simulation could begin. Due to the lead time on receiving test pieces and the time required to carry out testing within the already limited design period, values were used from the 3D Systems datasheet on DuraForm GF of a yield strength of 27 MPa and Young's Modulus of 4068 MPa. The Poisson's ratio used was 0.4, based on the Poisson's ratio of other SLS printed Nylon-12 materials. It was assumed that the generous safety factor and conservative approach to design would compensate for the anisotropy of the material, but in hindsight this was an unwise choice and time would have been better spent on research and material setup and is detailed later in this report.

Boundary conditions for each type of simulation were determined from on-track data in MoTeC i2Pro, and Ricardo 1D simulation, to ensure the load cases were realistic and that the part would not fail on track. Finally, a preliminary safety factor of two was targeted for the system. The conservativeness of the safety factor was a result of the uncertainties of implementing the SLS manufacturing method for the first time, and the simplifications made when setting up the model.

Unfortunately, within the time constraints imposed by the 2-month MMS design period, a working CFD model was not achieved until a few days before 'design freeze', when design work must cease, and outsourcing must begin. As such, it was not able to be used for design purposes, but rather as a check to ensure no separation was occurring in the restrictor-diffuser section. This was identified as an area of further refinement, and thus the full set-up and final results are discussed later in this report.

5.8.1 Boundary conditions

In determining the FEA loading conditions, on-track data collected from M18-C was consulted. This is analysed in MoTeC i2Pro where the output of different sensors can be displayed with reference to time or distance to accurately show vehicle state at any given moment. The data used for FEA is shown in Figure 21 and 22 below.

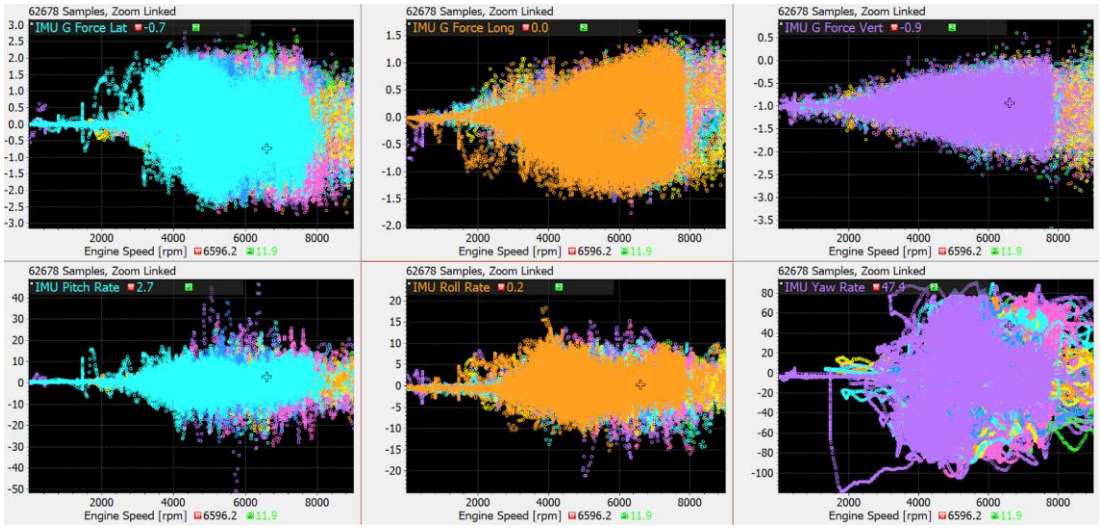

Figure 21: Acceleration vs engine speed scatter plots for an endurance event

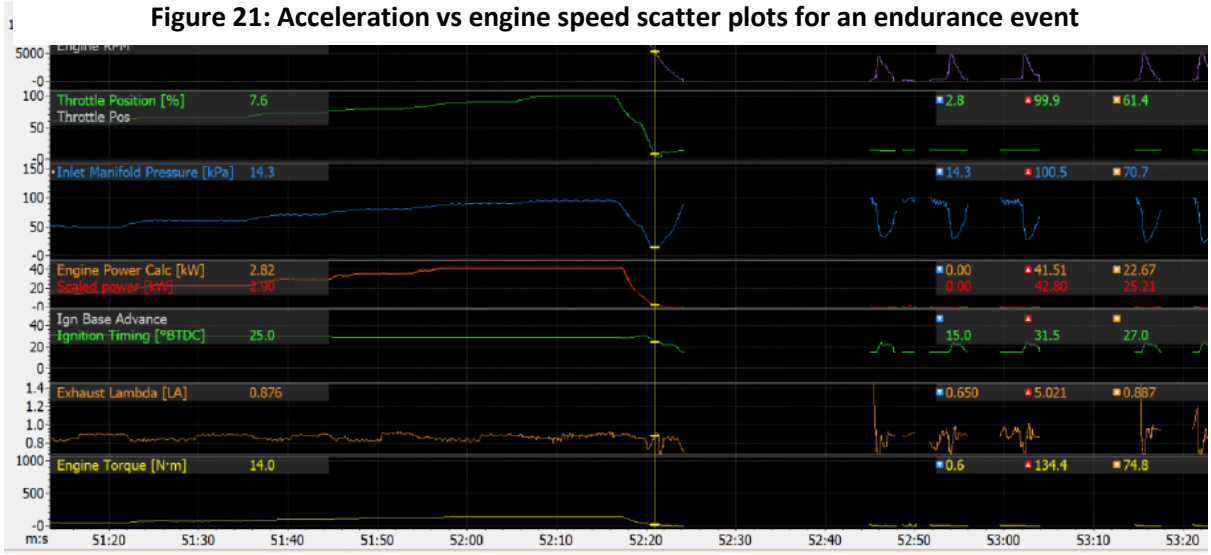

Figure 22: Traces of throttle position, engine speed and MAP

From this data, it was determined that the vehicle acceleration load case used would be 2.6g lateral, -1.9g longitudinal and 5g vertical. It was also decided that the pressure within the intake would be simulated at absolute vacuum. While this was a conservative choice, it was deemed necessary due to the aforementioned simplification of setup and the team's inexperience with the manufacturing method.

For the CFD boundary conditions, Ricardo was used with mass airflow sensors placed throughout the intake system, with the results of this shown in Figure 23. From this graph, it is apparent that the flow is the least transient near the throttle body, justifying the choice to only model the first portion of the intake system in the CFD model. From taking the average airflow at 8000rpm wide-open throttle, the outlet condition for CFD was determined to be 0.0583 kg/s, with an atmospheric inlet. As discussed prior, due to difficulties with implementing the model, it was not used to guide design in design period and was identified as an area of future refinement.

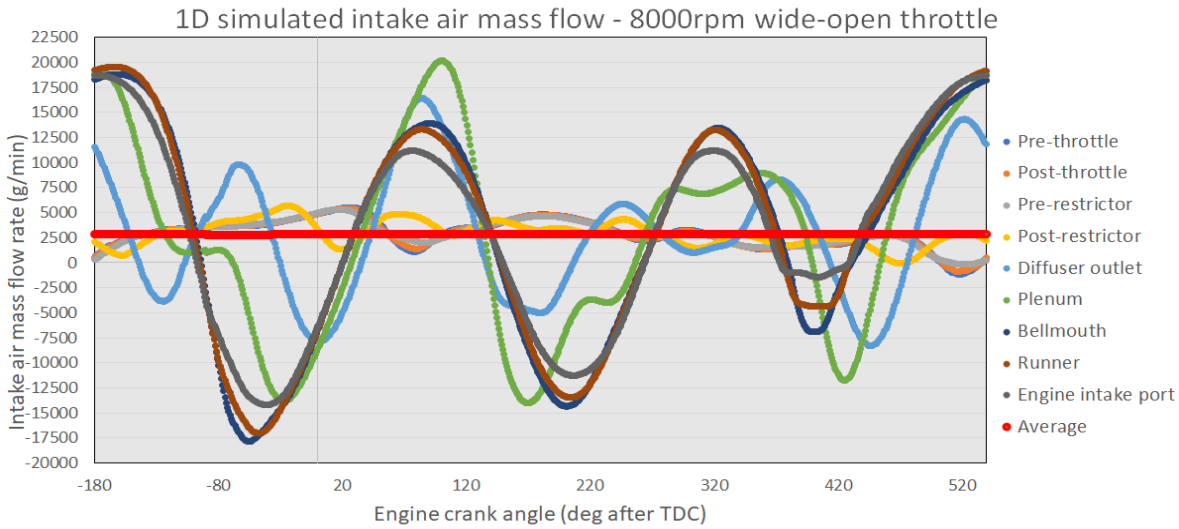

Figure 23: 1D simulated air mass flow

5.8.2 Mounting Solution

Due to the mounting of any system being a likely spot for stress concentrations and failures, as well as not having high potential for mass savings, it was decided that it was necessary to provide a robust mounting solution before structural optimisation could begin. Firstly, the mounting points on the chassis and the restrictor were chosen so that the CAD model could be produced. It was found that the two mounts directly to the chassis carried significantly more load than the mounts at the restrictor, to the extent where the nylon would yield. To rectify this, the mount was adjusted to incorporate a bonded aluminium insert to better distribute the load from the bolt hole. It is worth noting that because the bolt hole was 'fixed' in this setup, it was likely experiencing more stress than it does in reality, where it is attached to a rubber mount. The FEA guided the use of a thicker wall in the plenum mounts, and the use of gussets at the restrictor flange. Screenshots of these mounting solutions are shown in Figure 24.

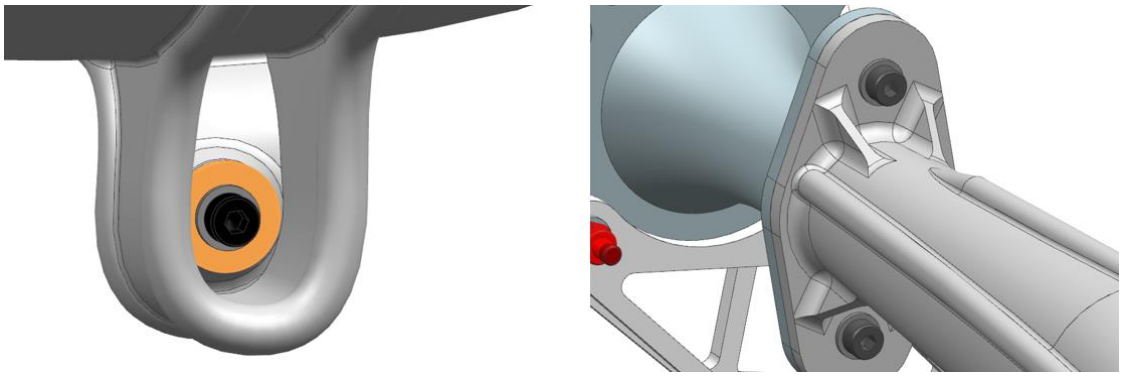

Figure 24: Plenum mount (insert highlighted) and restrictor flange mounts

5.8.3 Intake Structural Design

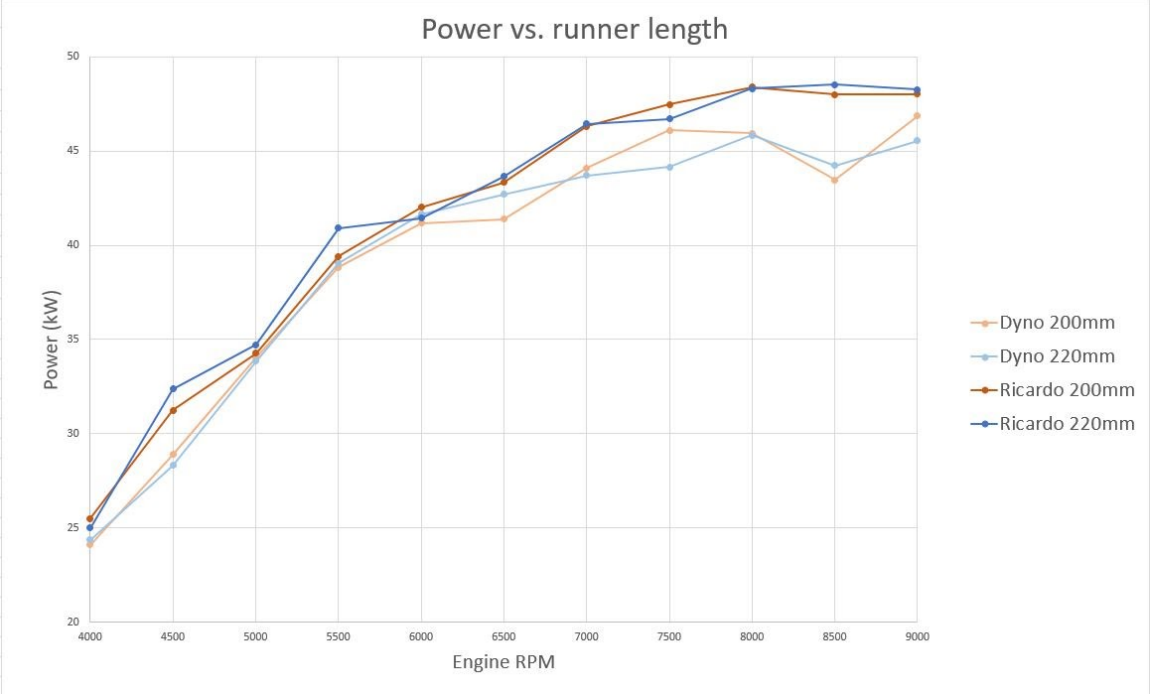

Figure 13: Power vs engine speed for 200 and 220mm runner lengths

With the mounting solution of the intake system determined, the next step in FEA was to design the structure of the system. Due to the need for the system to fit within the rollover envelope of the car, and package a 6-litre plenum, it was quickly determined that a 220mm runner would be unviable, as it would require the bellmouth to protrude almost halfway into the plenum. This is undesirable as it will need to draw a significant amount of air from behind the bellmouth, where it must turn through 180 degrees to enter the runner. This resulted in a change to a 200mm runner, with the simulated difference in power shown in Figure 25 determined to be of negligible effect.

Another effect of packaging a 6-litre plenum within rollover was the elliptical shape that the cross section needed to take. The more convex the geometry, the stronger it is under vacuum, and hence needing to package the 6-litre plenum necessitated the use of an additional stiffening structure, as a homogenous wall thickness design would not be able to pass stress requirements without being unfeasibly heavy. The target mass of the printed system was 1.5kg, in order to not be heavier than the 2018 system.

The result of the need to add a stiffening structure resulted in the addition of ‘ribs’, an early iteration of which is shown in Figure 26. What can be seen from this picture is that the ribs take a substantial amount of stress from the surrounding area and concentrate it within the rib itself. This design has a maximum stress of over 40 MPa within the ribs themselves and hence would fail under vacuum pressure. With ribs verified as a viable way to increase the stiffness and decrease stress through the system, they were further explored.

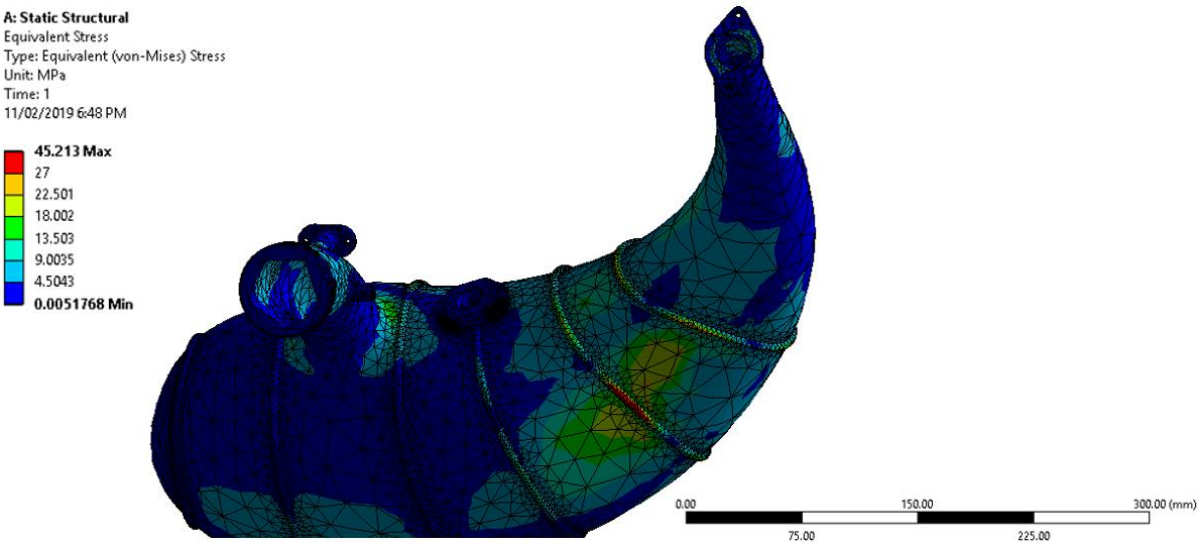

Figure 26: An early iteration of the 'ribs' concept. Maximum stress of 45 MPa

In an iterative technique, ribs were added or enlarged to address stress concentrations found within the FEA. This resulted in ribs of variable thicknesses, depending on the stress they experienced and the implementation of longitudinal ribs. Some consideration for aesthetics were made also, with the mounts incorporated seamlessly with ribs that went around the whole plenum, and ribs included on the diffuser as to avoid looking out of place. While the F-SAE competition is primarily performance and knowledge based, there are still 5 points based on vehicle aesthetics and gaining and retaining sponsors is crucial to the success of MMS.

Through this iterative design process, the final result is shown below in Figure 27. This has a peak stress of 24 MPa, but this is highly localised at a fixed constraint and as such was not deemed an issue. The highest stress in the rest of the system was approximately 16 MPa, with the vast majority being of a much lower stress than that. Maximum deflection was approximately 1mm, with a uniform wall thickness of 3mm and an estimated mass of 1.5kg. Worth noting is that while the results suggest a lot more refinement is still available, due to a lack of trust in the accuracy of the simulation due to highly simplified and likely inaccurate material and model setups, and almost reaching the conclusion of the MMS design period, this was chosen as the finishing point.

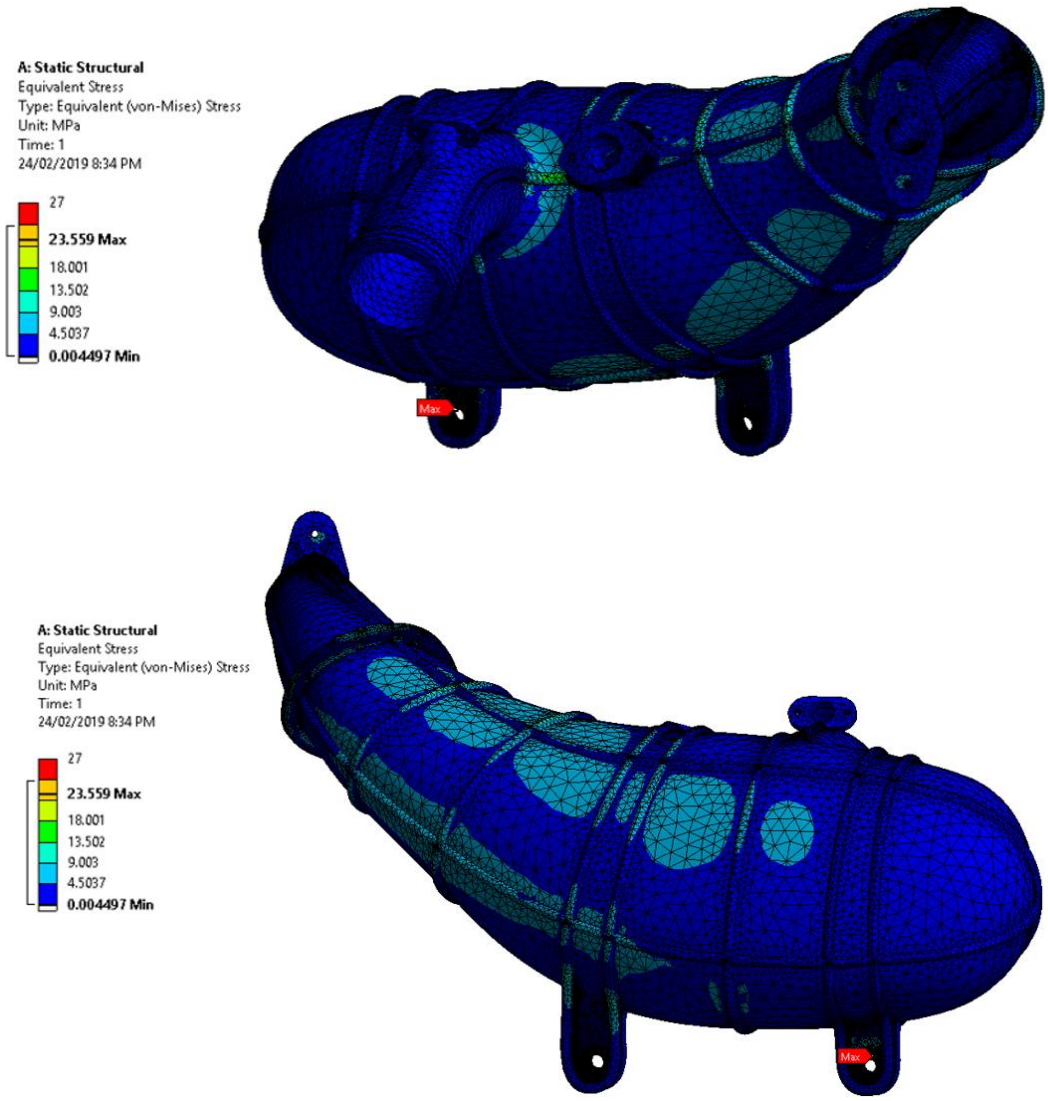

Figure 27: Stress distribution in the final intake design

5.9 Other Components

As well as the SLS printed portion of the intake system, there were still other components that needed to be designed for the intake to be a functional system. This includes mounting for the throttle body and air filter, restrictor design and restrictor mounting.

An air filter is one of the components in the intake system that contributes to the overall pressure loss (Heywood, 1988) and is required to prevent contaminants entering the combustion chamber and reducing the engine's lifespan. In order to minimise the pressure loss, an air filter should be chosen with the minimal possible restriction, meaning the medium must be as free flowing as possible, while the surface area should be as large as possible. For this reason, a UniFilter 63mm air filter was selected as it was the largest filter that would fit in the throttle body location. To mount the air filter and reduce the pressure loss into the throttle body, a bellmouth was designed to be SLS printed with similar internal geometry to that on the runner, with appropriate profiling to mate correctly with the air filter. This is shown in Figure 28.

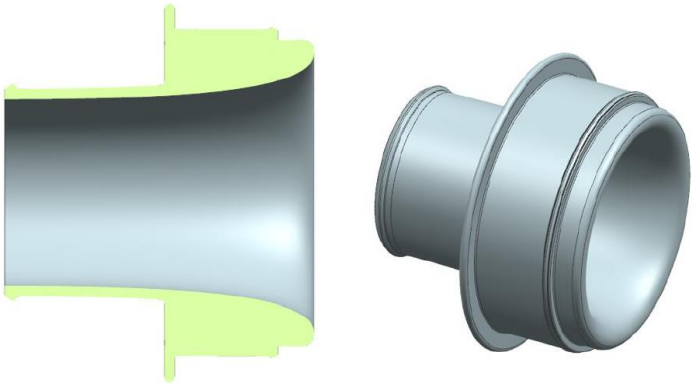

Figure 28: Filter bellmouth

Crucial to rules compliance and minimising the pressure losses in the system, is a well-designed restrictor. This should converge and diverge in such a way that the air loses the minimal amount of energy possible and stays attached through the transition into the diffuser. Originally, this was intended to be guided by CFD but due to difficulty in having the model reliably working on time, was guided by following best practise instead. This meant having transitions be as smooth as possible, with the restrictor throat being slightly less than 20mm to satisfy rules, and a gradual transition out to the maximum divergence angle of 3.5 degrees. To be able to interface with the ETB and printed diffuser, the ends of the restrictor were designed to press-fit into flanges. This is because machining the restrictor and flanges in one part would be highly expensive and complicated, while welding components together could cause distortion and prevent sealing between parts. Also, this method of restrictor mounting has been used in 2017 and 18 with great success.

Figure 29: M19-C restrictor

The flanges that the restrictor press fits into serve the purpose of mounting the restrictor to the throttle body and diffuser, as well as allowing for the connection to be sealed. To ensure a repeatable and reliable seal between parts, O-rings are used, with the O-ring grooves of the flanges sized from standard conventions. The flanges were designed to be made from 4mm aluminium, so that the press depth of the restrictor would be sufficient to bond and seal. The flanges are shown in Figure 30.

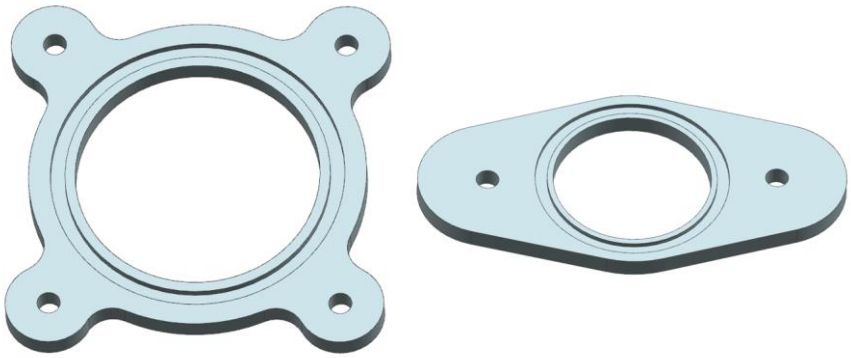

Figure 30: ETB (left) and diffuser (right) flanges. Note the O-ring grooves

As with all other structural parts on the car, the aim for the ETB mount was to be structurally sound and as light as possible. To achieve this, a trussed design was produced, to be laser cut from 3mm aluminium and welded to manufacture the part. This would mount to the chassis by three glue-on M6 studs, and mount to the bottom two mounting holes of the throttle body by two M4 bolts. By rules, all parts of the intake system that mount to the chassis need to incorporate some form of vibration isolation (Society of Automotive Engineers, 2019), to prevent relative movement of the engine, intake system and chassis resulting in a failure. For this reason, it was decided that a piece of rubber sheet would be fastened between the chassis and ETB mount to satisfy rules.

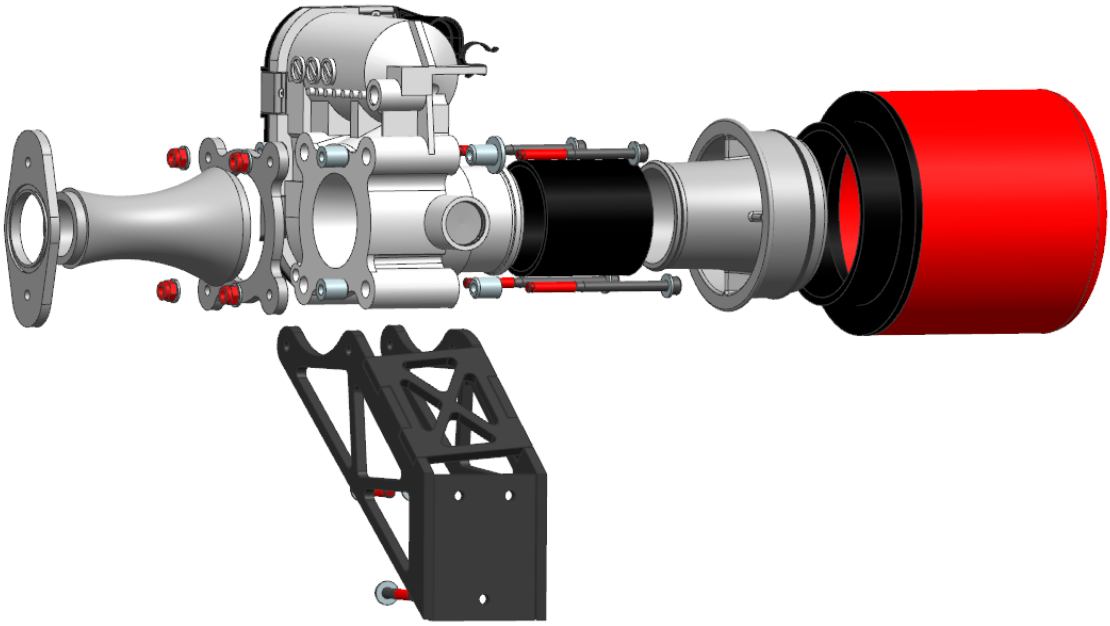

Figure 31: Exploded assembly of non-printed parts. Note the trussed ETB mount

5.10 Final Design

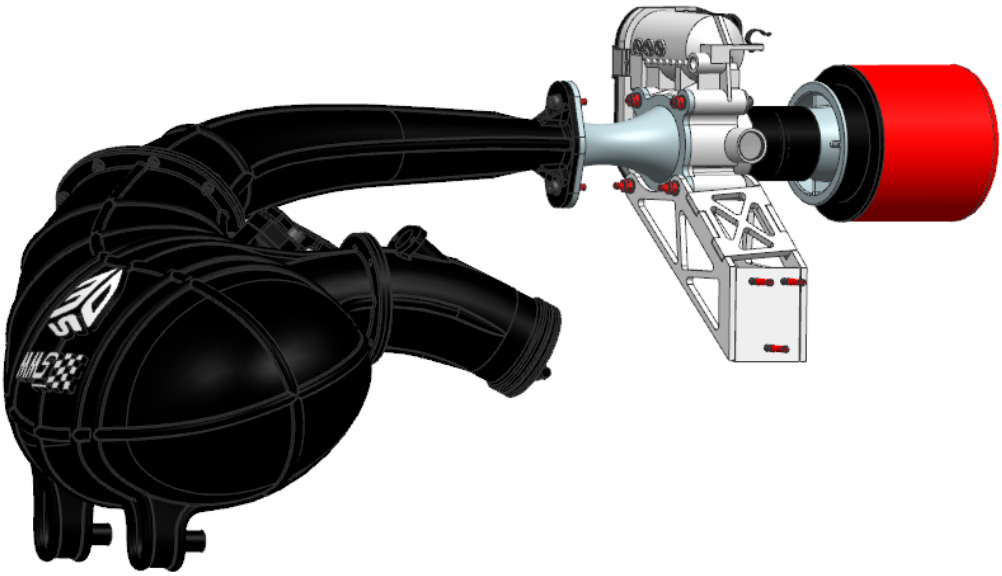

Figure 32: Entire intake system in CAD

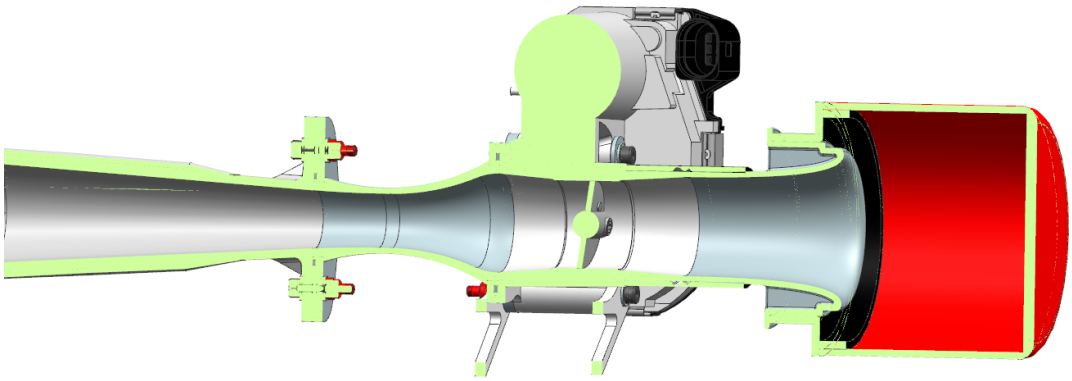

Figure 33: Internal geometry through the first portion of the intake system

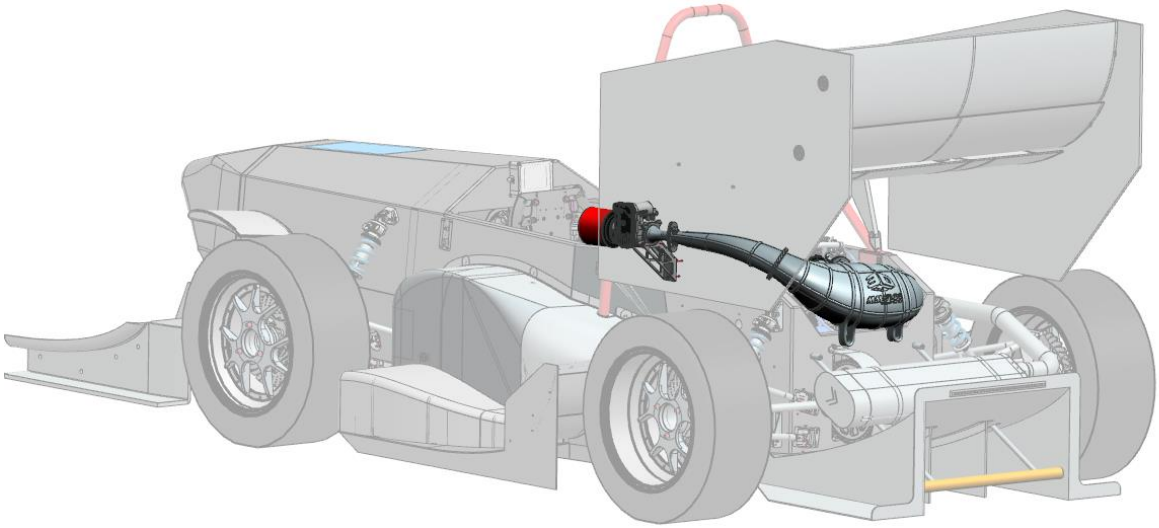

Figure 34: Intake packaging on M19-C

Pictures of the final system, internal geometry of the first portion of the system, and its positioning on M19-C is shown in Figures 32-34. The part passes rollover by approximately 15mm, and through use of the unique stiffening structure, has a simulated maximum stress of 16 MPa within the plenum and a maximum simulated deflection of 1.2mm through the flattest part of the system. The side-mounted concept ensures a low centre of gravity compared to other concepts explored, and the throttle body is positioned such that it receives cool air, away from the radiator outlet. The final estimated system mass was 2.8kg, with a simulated peak power of 48.4 kW and peak torque of 68.2 Nm.

6. MANUFACTURE

The manufacture of the printed part of the intake system was outsourced to 3D Systems, and the machined parts manufactured by either the mechanical engineering workshop or by team members. The total time from finishing the design of the part, to having a completed system on the dynamometer was approximately 6 weeks.

The most crucial part of the outsourced 3D printing process is that the files are exported in the highest resolution possible and are thoroughly checked for errors by multiple people. The parameters to consider when exporting a part for 3D printing is the chordal and angular tolerances. Because the STL file used for 3D printing models surfaces as triangles, it is necessary to define these appropriately to avoid a 'faceted' appearance on the curved surfaces. Chordal tolerance refers to the maximum distance between a flat surface and the original curved surface, and angular tolerance limits the angle between the normals of adjacent triangles. Typical values recommended for these are a chordal tolerance of 0.001mm and an angular tolerance of 15 degrees, with visual representations of these tolerances shown in Figure 35.

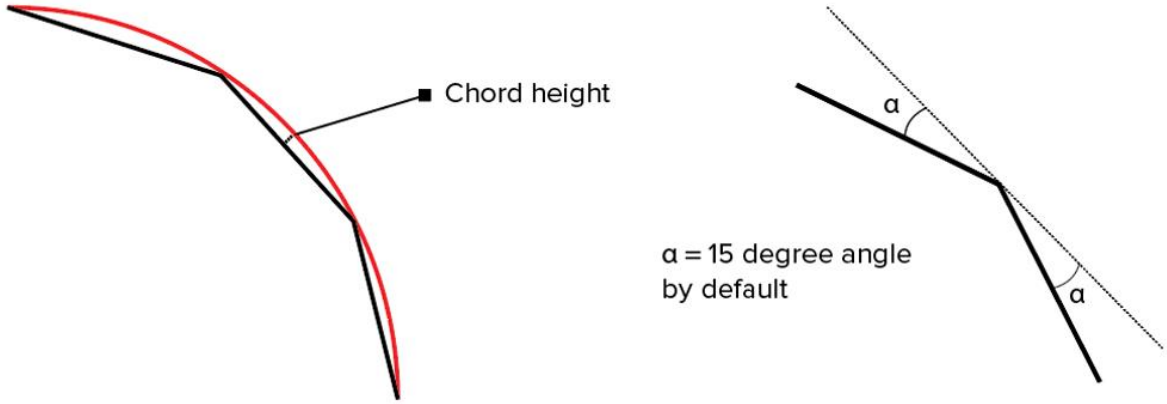

Figure 35: Visual representation of chordal tolerance and angular tolerance (3D Hubs, 2019)

Upon receiving the intake parts back from 3D Systems, it was found that the captive nuts, and bolts into bolt holes didn't fit as well as expected. This is likely due to the resin coating pooling in these areas, and hence they should be enlarged in future. Due to the limited time available for dynamometer calibration before the electric powertrain needed to use the dynamometer, it was decided to only smooth the inner surface of the filter bellmouth and not to post-process the diffuser and runner. In future this should be done so that the benefits can be quantified by physical testing.

All machined parts required technical drawings to be made for them and STEP files made for the CNC (computer numerical control) machined parts. A H7/p6 interference fit was elected for the pressed components and tolerances on the drawings adjusted accordingly. No issues were encountered with the machined parts in the system. The technical drawings for these pressed parts are included in Appendix B.

When all of the parts were received, the machined portions were press fit together, and the intake sections bolted together, using a fuel resistant RTV as the gasketing material. Finally, the system was mounted to the dynamometer, as shown in Figure 36

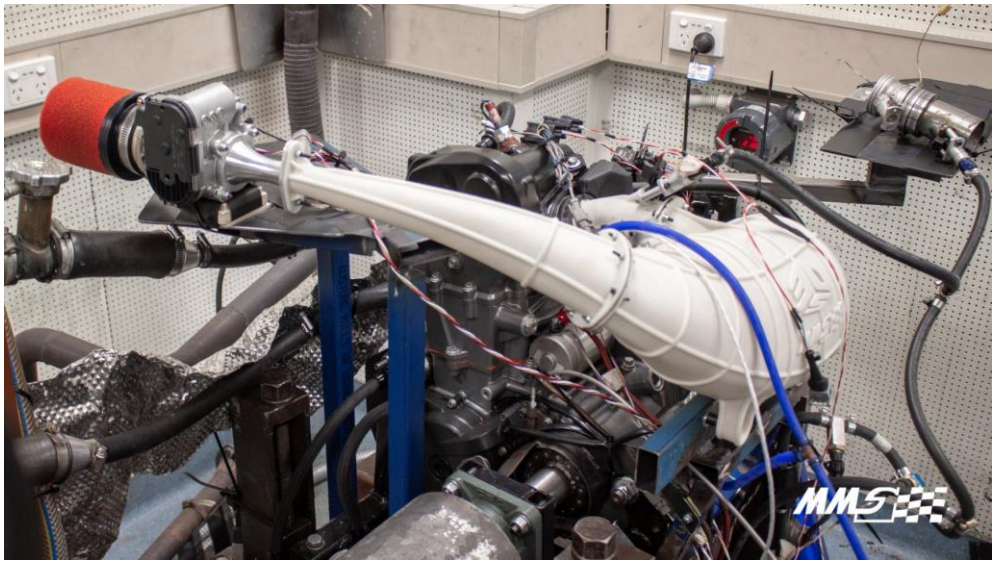

Figure 36: 2019 intake system mounted on the Monash dynamometer

7. DYNAMOMETER TESTING

7.1 ETB Implementation

Because MMS had no experience with using or tuning an ETB before, it was important to first validate and understand the use of an ETB to throttle air to the KTM 690 Duke R. This required manufacturing a flange and adapter to mount the ETB to the 2018 testing intake before the 2019 system was ready. From here, recommended values within M1 Tune (MoTeC M150 tuning software) were used to calibrate the ETB. Figure 37 shows minimal delay occurring between the input request (throttle pedal), output request (throttle aim) and output result (throttle position).

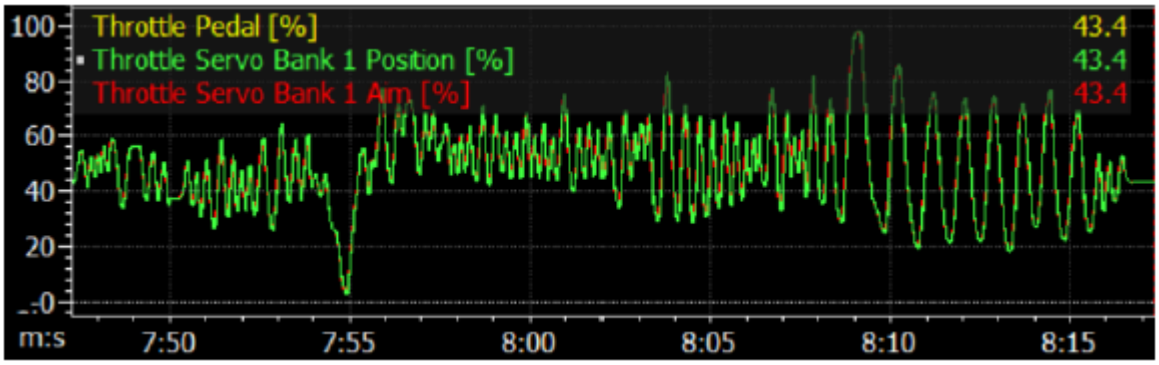

Figure 37: Throttle pedal, aim and position traces as viewed in i2 Pro

Following this, the ETB was then used to successfully throttle air to the engine on the dynamometer, with throttle profiles for starting and idling created. This confirmed one of the key advantages of the ETB, which is to start at a higher throttle position and then ramp down to a low idle throttle position, in the interest of easier starting and lower engine speed at idle. These profiles can also be scaled with engine temperature, to further increase ease of starting and idling.

7.2 Calibration

Once the intake system had been manufactured and assembled onto the dyno, the engine needed to be calibrated and tuned to determine appropriate fuelling and ignition timing. The process for this was that once the engine was starting and idling reliably, a conservative ignition map was put into M1 Tune, of approximately 20 degrees of ignition advance (before TDC) at all engine speeds and MAP sites. The engine was then be able to run safely at all sites, while the fuelling table (Engine Efficiency in M1 Tune) was tuned so that the lambda sensor correlated with the target lambda value of 0.9. An example of the Engine Efficiency table for M19-C is shown in Figure 38.

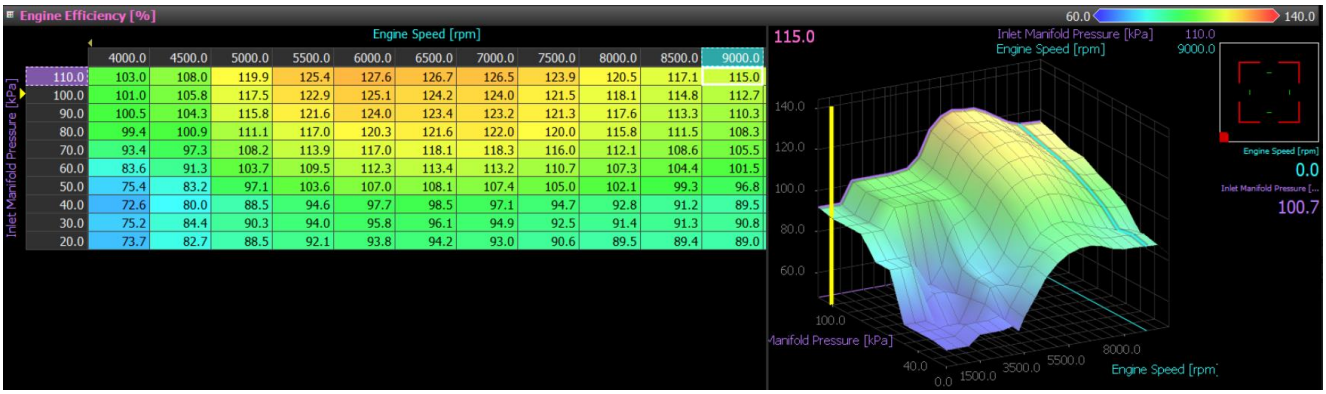

Figure 38: Engine Efficiency table in M1 Tune

Once a correct fuelling table was calibrated, ignition sweeps were then conducted from 4000-9000rpm at manifold pressures of 40, 70 and 100 kPa. The MoTeC software has the ability to interpolate between tuned sites and this was deemed a suitable resolution for the tuning process. The target for ignition tuning is to find maximum brake torque timing, MBTT. The level of ignition advance that this corresponds to is the highest torque output for a given speed and manifold pressure site, and hence the highest efficiency for the engine. Past MBTT, the piston must exert a higher amount of work on the combustion mixture to combust it, than is gained by having a higher peak cylinder pressure. An example of an ignition sweep to and beyond MBTT is shown in Figure 39, where power clearly increases and decreases on either side of MBTT.

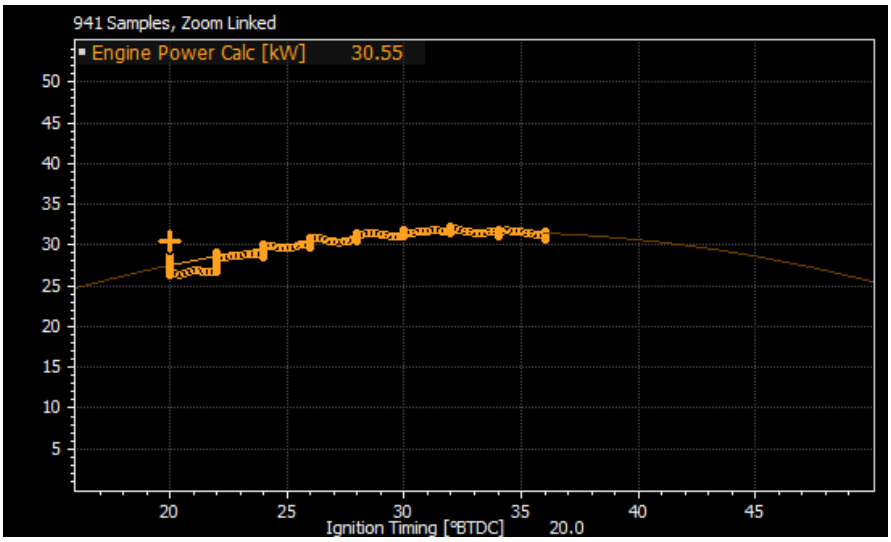

Figure 39: Ignition sweep at 8500rpm, 70 kPa MAP

Another limit that can be reached aside from MBTT is the knock limit. 'Knocking' of an engine occurs when as the flame front travels out from the spark plugs, an area of unburnt mixture in the combustion chamber reaches a high enough heat and temperature that the intake charge spontaneously ignites in that area, resulting in high pressure waves being created in the cylinder that make an audible high pitched sound and can quickly damage an engine. Knock is most likely to occur at and around the peak torque site, as this is where maximum volumetric efficiency is achieved and therefore where in-cylinder pressure reaches the highest value. M19-C is knock limited from approximately 5500-7500rpm and was able to be tuned to MBTT everywhere else. Once the ignition table was finalised, fuelling was re-checked and adjusted where necessary.

7.3 Results

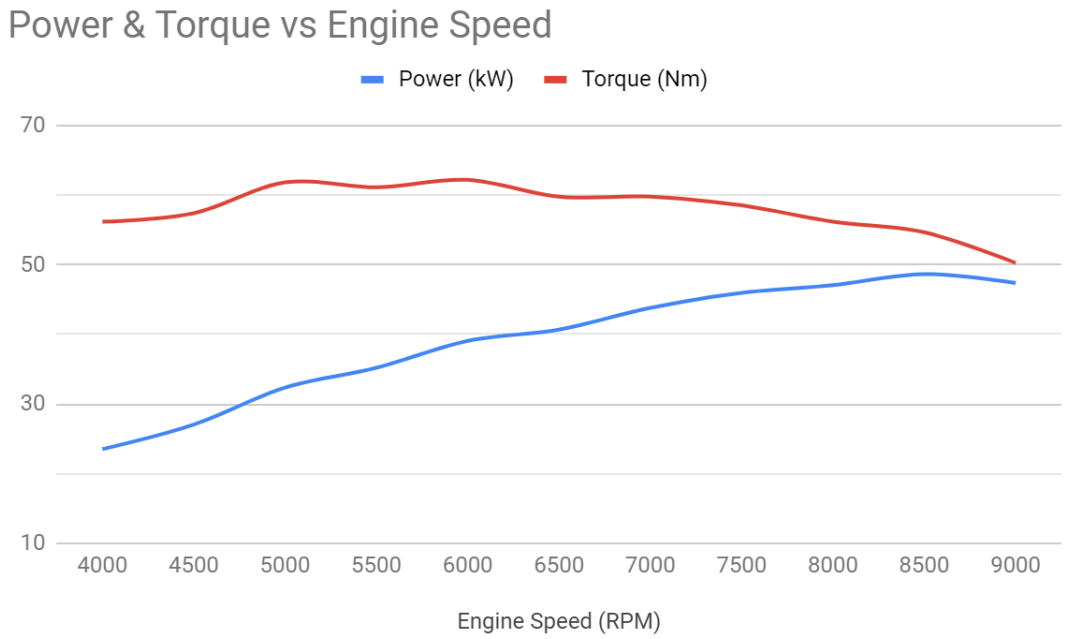

Figure 40: Final power and torque curves for M19-C

Through this dynamometer testing, power and torque curves for M19-C and the new intake system were able to be produced, shown in Figure 40. The peak power of 48.6 kW matches simulation to

within 0.2 kW, however the peak torque of 62.2 Nm differs by approximately 6 Nm from the simulated value. The reason decided for this discrepancy was investigated by viewing dynamometer data gathered from 2017 through to the end of 2018, the peak torque output of the engine used on the dynamometer decreased considerably by approximately 6 Nm, where this is likely due to engine wear. This correlates well with the delta between the simulation and dynamometer data. Another key parameter of engine performance is brake specific fuel consumption (BSFC). BSFC is measured in g/kWh and is a measure of the grams of fuel required to produce one kWh. Ricardo suggested that the 2019 intake system should have an average BSFC of 15 g/kWh less than the 2018 system, and preliminary calculations correlate well with this difference, with the curve made from these preliminary calculations shown in Figure 41.

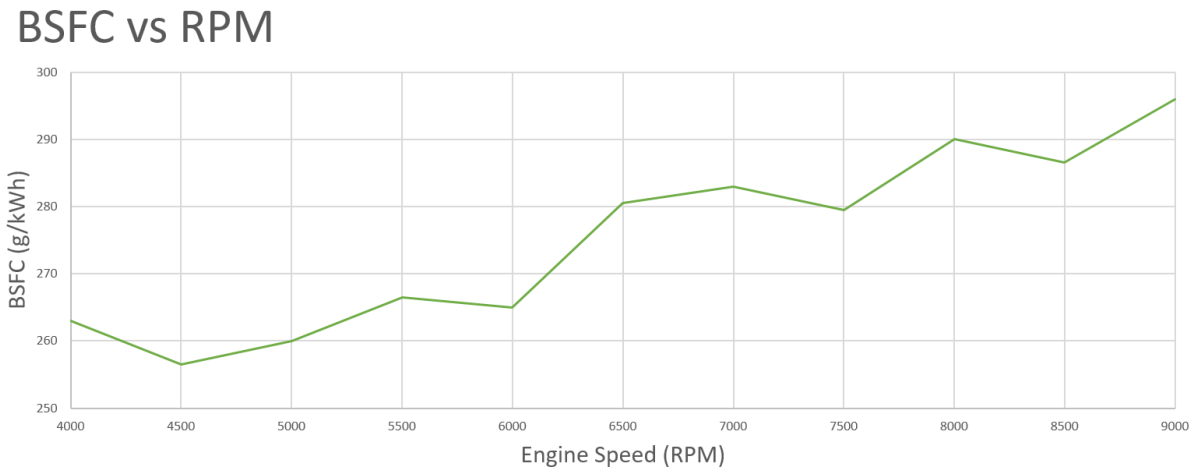

Figure 41: BSFC vs engine speed

Another point of interest is that all data through 2017 and 2018 was gathered using a simplified 'dyno' intake. This did not have the 120 degree elbow into the plenum or the curves runner that the intake system on M17-C and M18-C had, therefore the power output of the cars was likely reduced compared to the dynamometer results as there would have been less pressure drop in the dynamometer intake than in reality. In comparison, as all tuning in 2019 was done with the same system that was implemented onto the car, the results are much more comparable.

8. On-Car Integration and Testing

With the combustion powertrain successfully calibrated on the dynamometer, the engine had to be removed and mounted in M19-C, and the electric powertrain moved onto the dynamometer. This meant that focus shifted to implementing the system onto the car in a rules-compliant manner. The only remaining part to be manufactured at this point was the ETB mount. It was jigged and tack welded on the car with the intake system mounted appropriately to ensure a perfect angle and fit and was then seamed off the car.

The intake system was then painted for several reasons, firstly the system was extremely prone to picking up dirt from being touched and was extremely difficult to clean. In terms of contributing to the overall aesthetics of the car, the off-white printed colour, especially when dirty, would not represent the team or 3D Systems well. Finally, painting the exterior of the system provides another sealing layer against moisture ingress into the material and increases its reliability. The painting of the system was completed using a 2-pak paint supplied by Valspar.

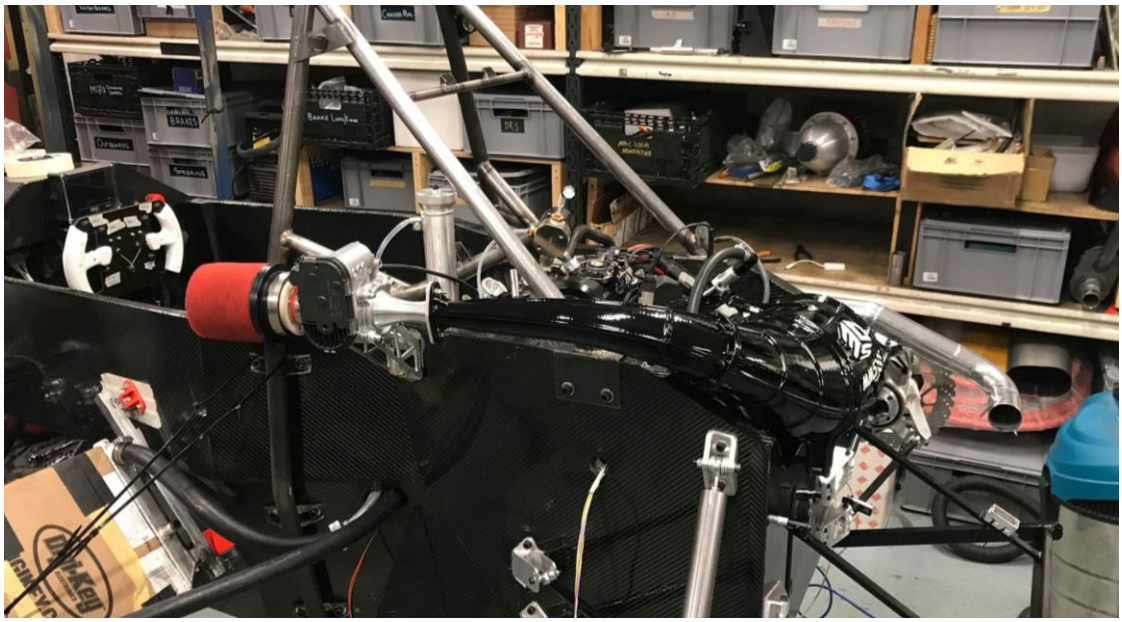

Figure 42: Intake system installed on M19-C

The system was then implemented onto the car in the same form that it was on the dynamometer, and hence the car started very easily. Sensing of pedal position was achieved using two linear potentiometers on the pedal, with a resistor in line with one of them to achieve the rules-compliant offset between signals. From here, further idle control was undertaken to further increase stability of idle and ease of starting. All of the plausibility checks that are required by rules (Appendix A), such as the throttle not reaching its target position for an extended amount time or losing signal to one of the throttle position sensors, were implemented in M1 Build (the M150 firmware program).

Finally, the hardware BSPD was implemented onto the car, a circuit that latches the shutdown circuit of the car open if it detects hard braking and the throttle being open at the same time, or if the signals from either of the TPS's or brake pressure sensors. This has proven challenging, with several iterations of the circuit board needed to be created and debugged, but a rules compliant solution was eventually reached.

On track tuning so far has been limited to shifting, adjusting throttle profile based on driver feedback, and the implementation of the transient fuel film model. Shifting, and downshifts in particular, are considerably smoother than in 2018. This is due to the ETB's ability to be 'blipped' on downshift, which better matches the engine and gearbox speeds when the clutch is reengaged. Another adjustment made has been the move from a linear pedal position to throttle position ratio, to a more exponential profile. This was done based on driver feedback on track, to increase the resolution of the throttle at lower, more sensitive positions, until they were happy with the drivability of the car. Further throttle profile tuning is planned for the skid pad event, where a high

resolution between 10-25% throttle position should greatly improve the driver's ability to maintain a high steady state performance.

The closed-loop fuel film model compensates for the transient manifold pressures and engine speeds seen on track by the car, which are unable to be tuned on the steady-state dynamometer. During intake operation, a film of fuel forms on the walls of the runner and intake ports. In a steady-state situation, this film reaches an equilibrium with the amount of fuel being added and evaporated from it so that its volume remains the same. When manifold pressure and air flow rate (proportional to engine speed) change, so does the fuel volume in the film. Hence, the M150 fuel film modelling can predict the volume of the fuel film at any operating site and adjust the duty cycle of the injector accordingly to maintain a stable lambda and improve the drivability of the car.

9. FURTHER REFINEMENT

Later in the year, after the system had been tested and integrated onto the car, it was decided that time would be best spent refining the simulations, in particular the setup, to improve their accuracy so that the part could be refined further in future. Thus, this was the focus of mine, William Jenkin's and Jack Martin's MEC4407 (Design 3) project. As the majority of the work is in those submissions, this section of the report just serves as a summary of the progress made and the work done.

Firstly, the material setup in ANSYS FEA needed to be properly validated, as the anisotropy had not been tested or considered in the first setup. For this, a test piece was designed to be tested under vacuum, so deflection of the part could be measured while pressure was varied in 5kPa increments. This would then allow for a comparison of the current FEA setup to physical results, and the calibration of the material model to match physical results, and these plots are shown in Figure 43.

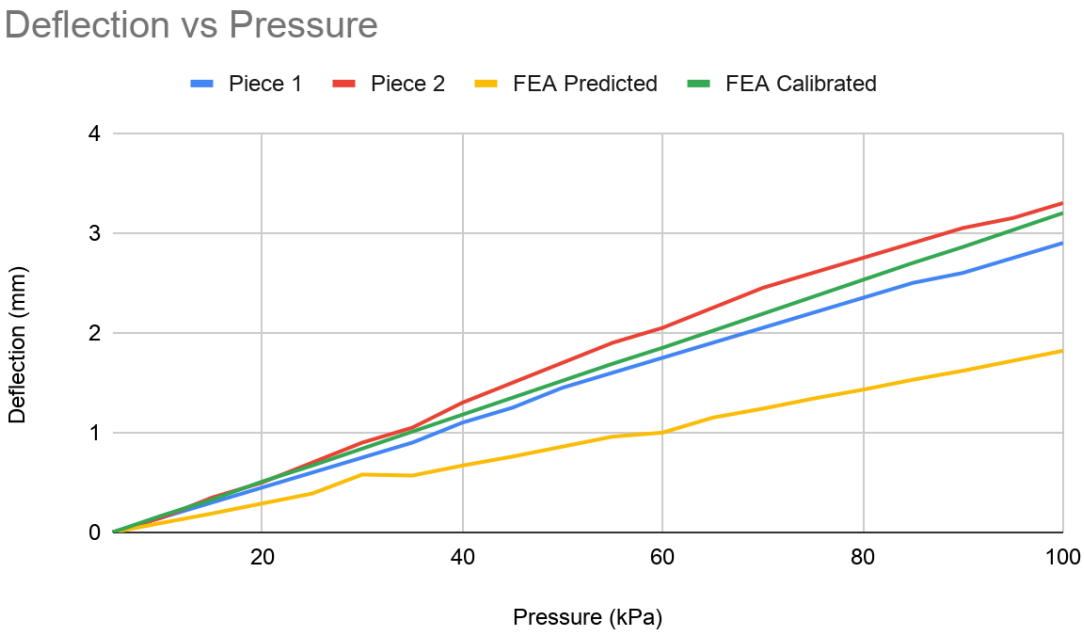

Figure 43: Deflection vs vacuum pressure for the physical testing piece

The decision was made to continue defining the material isotropically, with mechanical values taken in the weakest (print) direction. While an anisotropic model would be most accurate, the weaker isotropic model is more robust, as regardless of the orientation of the part in the printer, it will be structurally sound. These tests and further research, resulted in Poisson's Ratio changing from 0.4 to 0.35 (Cano et al., 2018) and the Young's Modulus being adjusted from 4068 MPa to 2400 MPa. The result of this was that the simulation of the test part correlated with the physical testing much more accurately. In addition to this, tensile yield strength was reduced from 27 MPa to 25MPa, based on three-dimensional data given on glass-bead filled nylon-12 by other suppliers. The final material setup is shown in Appendix C.

The boundary conditions and fixtures for the model were also addressed. This resulted in the plenum mounts being modelled as springs to the chassis, with stiffnesses of 98.1 N/mm based on their datasheet (Mackay, 2015). The rubber booty to the engine was also modelled as a spring and the bolted connections to the diffuser modelled as such. The full FEA setup is shown in Appendix C. Finally, mesh size and type was investigated and it was determined that for maximum accuracy within a reasonable timeframe and to avoid issues such as shear locking a 4mm 8-node, second-order, quad-shaped, full-integration element should be used, with refinement at the mounting points. Unfortunately, this mesh has not been implemented onto the current intake for comparison, but the rest of the setup has been applied and the results of this are shown in Figure 44.

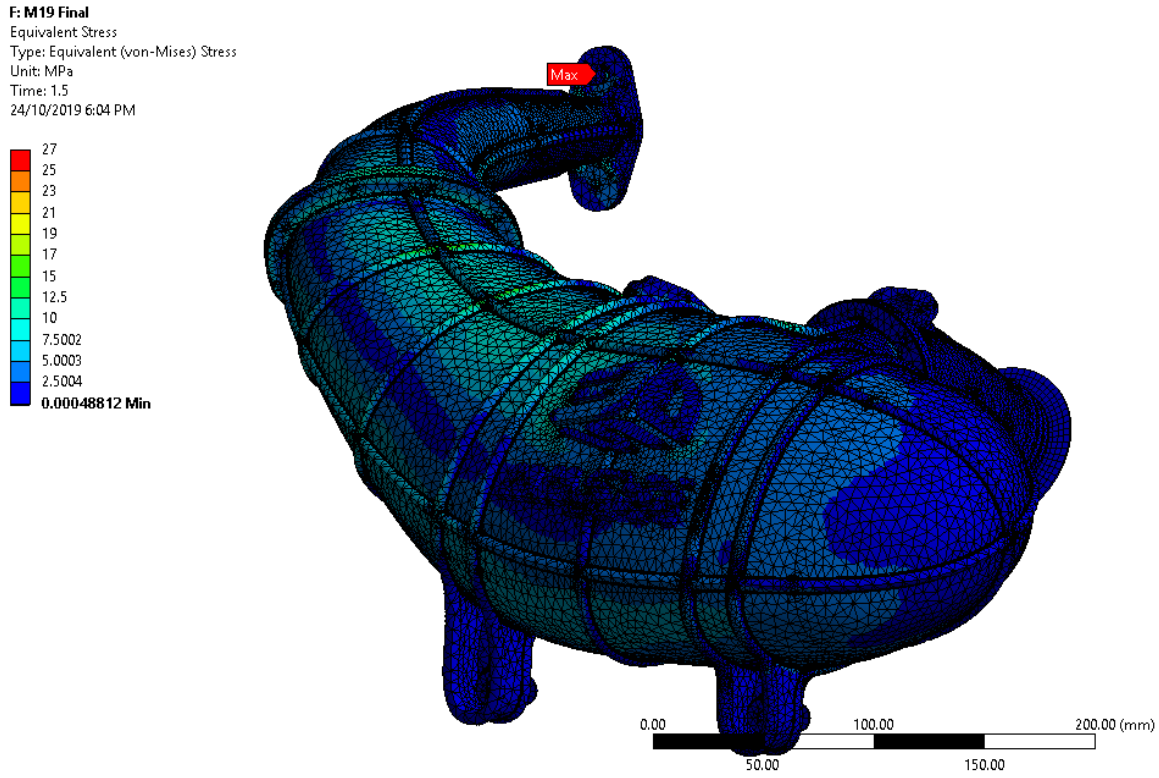

Figure 44: Refined FEA intake stress distribution

The maximum stress seen within the plenum itself stayed relatively similar, with a maximum of approximately 18 MPa seen at the peak of one of the stiffening ribs. Substantially different from the original simulation however is the stress distribution through the part, showing very low stress through the plenum mounts. This suggests that they were over-designed. The part was also able to move in a much more realistic manner compared to having fixed mounting points, with the movement of the plenum mounts detailed in Figure 46. The deflection in the part itself also matched that which was observed during operation to a more realistic degree, with up to 2mm of plenum deflection.

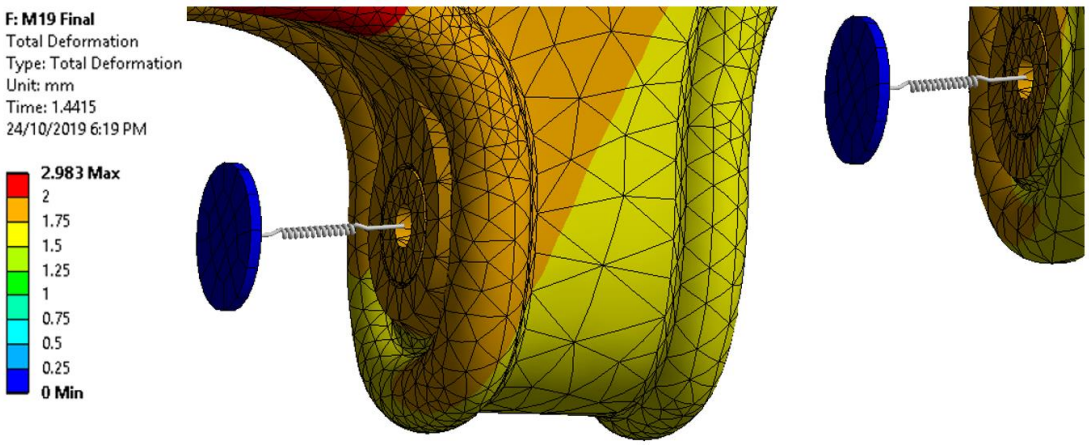

Figure 44: Displacement of mounts with soft mounting implemented

Due to the CFD model not producing any results until the end of design period, it was decided to invest in making it work, and determining if it could be used for future designing. The model setup converged on and the mesh setting used are all listed in Appendix D. The simulation still had a considerable (approximately 10%) error in convergence, but through comparisons with geometries known to be poor, was determined to be a useful tool to ensure designs wouldn't cause excessive flow separation. The velocity planes for the 2019 intake system, and a system utilising an orifice plate are shown in Figure 46, with simulated pressure drops at the diffuser outlet of approximately 4 kPa and 20 kPa respectively. Some separation can be seen in the 2019 system as the diffuser geometry starts to change to 'wrap' over the chassis wall, but the pressure drop was unchanged compared to other geometries that took longer to separate.

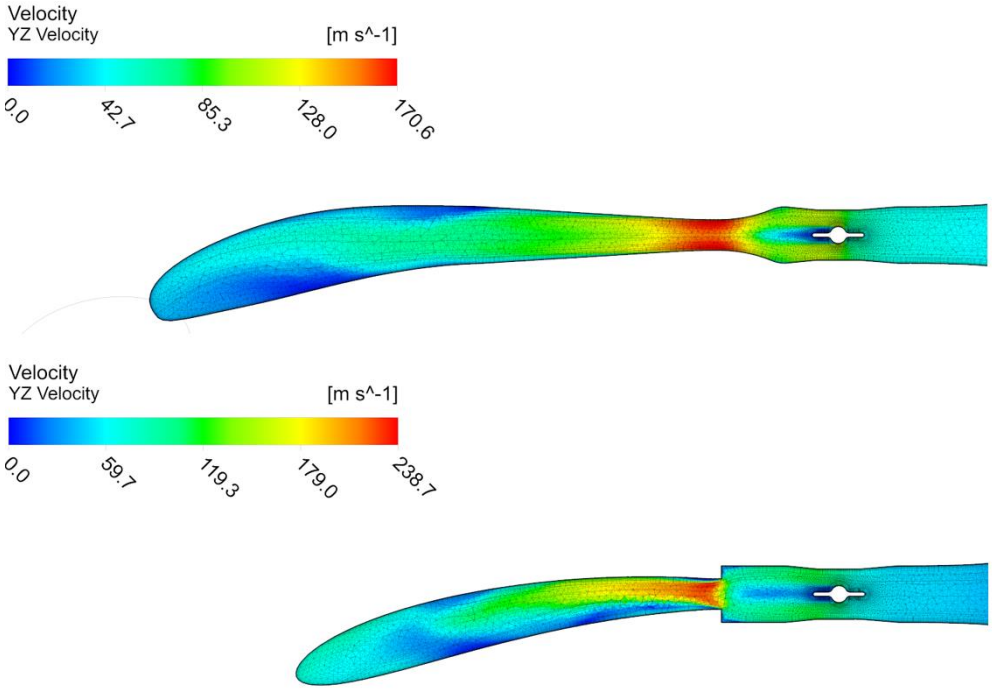

Figure 46: Velocity distributions through M19-C's intake and an orifice plate system

The further refinement undertaken will therefore allow future part designers to optimise the intake system design to a much greater degree, with high potential for improving the structure of the part, but minimal gains to be made in improving the flow geometry through the first portion of the system unless the CFD model can be further improved.

10. RECOMMENDATIONS

The recommendations made by this report to MMS, and specifically the future part designers, is to improve the accuracy of the simulations, specifically the FEA so that future designs can be much more optimised than this one. Setup is everything and time should be dedicated to the setup before any substantial design work is undertaken.

To improve the material setup further, standardised physical testing of printed samples printed in all orientations should be conducted to empirically determine the tensile strength, bending modulus etc. This will allow for a holistic understanding of the material in a 3D sense an improve confidence in the design. The boundary conditions of the FEA could be improved also, by more accurately

modelling the rubber boot connecting the runner to the inlet port of the engine and introducing transient loadings of acceleration and pressure over a very small time frame to realistically simulate conditions on the car.

As discussed in the previous section, improving the mesh quality used will also ensure that simulations are more accurate. Improved CAD techniques, such as the implementation of variable wall thicknesses, optimised rib geometry that eliminates the stress concentrations seen in the current system and investigating a way to add stiffening structure in a less ad-hoc manner will improve the performance of the final product.

With regards to CFD, as was discussed in the further development section, if good engineering practise is followed with regards to a correct restrictor and diffuser geometry, the system will already be at the point of diminishing returns. Hence, it is not recommended that the CFD model be pursued further, but rather used as a tool to 'sanity check', or verify, a design. It would be of benefit to validate the CFD model by pressure tapping the intake, but generally there are much more important things to be done within the system.

11. CONCLUSIONS

In conclusion, this project has resulted in the successful implementation of a rules compliant ETC system and SLS printed intake system onto M19-C. This has been validated to increase performance compared to the 2018 and 2017 fabricated systems, by increasing peak power by 1.5 kW at 8500 rpm and peak torque by 2 Nm at 6000 rpm.

The use of ETC has greatly improved the ease of starting and idling and has required no work to be done for maintenance at all. This was great improvement over previous years, where hours would be wasted every time the throttle cable needed adjusting. The throttle profile has also been modified from its original setting based on feedback from drivers, who find it more 'drivable' than a conventional throttle.

Further refinement of the simulation tools used for design at the beginning of the year has been undertaken and recommendations for further improvements to the tools made to future parts designers. This includes the recommendation to continue using FEA as a primary design tool, but to avoid using CFD apart from as design validation, as the point of diminishing returns can be reached by following good engineering practise for intake design.

One of the largest concerns with moving to a new intake concept for 2019 was reliability. With almost 700 km of racing completed so far, M19-C's intake system has performed reliably and without issue, confirming the viability of using ETC and an SLS printed system.

12. ACKNOWLEDGEMENTS

I would like to acknowledge the Monash Motorsport team for their continued support of the project and giving incredible opportunities to young future engineers.

I would like to specially recognise several people as well, firstly the team's academic advisor, Dr. Scott Wordley, for his mentorship throughout the project and his contributions to the team that are invaluable for its success. I would also like to thank William Jenkin and Matt Corallo for their mentorship regarding intake design and engine tuning, Jack Thomas and Jack Martin for their

assistance with CAD and CFD, and Tim Chang for researching and integrating the ETB into the Monash dynamometer.

13. REFERENCES

3D Hubs 2019, 3D Printing STL files: A step-by-step guide | 3D Hubs, 3D Hubs, viewed 24 October 2019, <https://www.3dhubs.com/knowledge-base/3d-printing-stl-files-step-step-guide/#rules>.

3D Systems 2019, Plastic Materials | 3D Systems, 3D Systems, viewed 2 August 2019, <https://au.3dsystems.com/materials/plastic>.

All3DP 2018, *All 10 Types of 3D Printing Technology in 2019*, All3DP, All3DP, viewed 25 September 2019, <https://all3dp.com/1/types-of-3d-printers-3d-printing-technology/>.

AT Power 2019, 28mm FS 20mm Restrictor Throttle Body., Atpower.com, viewed 24 September 2019, <https://www.atpower.com/products/28mm-fs-20mm-restrictor>.

AutoTap 2012, What the Home Mechanic Needs to Know about O2 Sensors, Autotap.com, B&B Electronics Manufacturing Company Inc., viewed 24 October 2019, <http://www.autotap.com/techlibrary/understanding_oxygen_sensors.asp>.

Blair, G & Cahoon, M 2016, SPECIAL INVESTIGATION: DESIGN OF AN INTAKE BELLMOUTH, viewed 18 September 2019, <https://www.pdf-archive.com/2016/01/30/velocity-stack-info/velocity-stack-info.pdf>.

Bosch 2019, 0 280 750 148 32mm Electronic Throttle Body ETB by Bosch, Bosch Motorsport Australia., viewed 24 October 2019, <https://www.bosch-motorsport-shop.com.au/electronic-throttle-body-32mm-bore>.

Brasfield, E 2015, 2016 KTM 690 Duke & 690 Duke R – First Ride Review + Video, Motorcycle.com, viewed 5 September 2019, <https://www.motorcycle.com/manufacturer/ktm/2016-ktm-690-duke-690-duke-r-first-ride-review.html>.

Cano, AJ, Salazar, A & Rodríguez, J 2018, 'Effect of temperature on the fracture behavior of polyamide 12 and glass-filled polyamide 12 processed by selective laser sintering', Engineering Fracture Mechanics, vol. 203, pp. 66–80.

Ceviz, MA 2007, 'Intake plenum volume and its influence on the engine performance, cyclic variability and emissions', Energy Conversion and Management, vol. 48, no. 3, pp. 961–966.

Claywell, M & Horkheimer, D 2006, 'Improvement of Intake Restrictor Performance for a Formula SAE Race Car through 1D & amp; Coupled 1D/3D Analysis Methods', SAE Technical Paper Series, viewed 25 October 2019, <https://www.sae.org/publications/technical-papers/content/2006-01-3654/>.

Cody Phillips Racing 2016, MoTeC M150 ECU - CodyPhillipsRacing.com, Cody Phillips Racing.

Formula Student Germany 2018, FSG: Results FSG 2018, Formulastudent.de, viewed 23 October 2019, <https://www.formulastudent.de/fsg/results/2018/>.

Heywood, JB 1988, Internal combustion engine fundamentals, 1st edn, Mcgraw-Hill Education, New York.

Integrated Publishing 2019, Actual Combustion Cycles, Tpub.com, viewed 17 August 2019, <http://www.tpub.com/engine3/en3-15.htm>.

Kariotakis, G 2011, 'Design and Manufacture of a Single Cylinder Intake System', Unpublished.

Mackay 2015, Flexible Isolator Catalogue, Mackay Rubber, Mackay Consolidated Industries, viewed 24 October 2019, <https://9198c40c-83e9-4d43-bf42-8056bee9b747.filesusr.com/ugd/17eaaa_00967e1ccf19420dbfc09a2b8fd1de79.pdf>.

MechStuff 2018, How does a 4 stroke engine work?, MechStuff, viewed 16 August 2019, <http://mechstuff.com/how-does-a-4-stroke-engine-work/>.

Negi, S, Dhiman, S & Sharma, RK 2014, 'Investigating the Surface Roughness of SLS Fabricated Glass-Filled Polyamide Parts Using Response Surface Methodology', Arabian Journal for Science and Engineering, vol. 39, no. 12, pp. 9161–9179.

Norizan, A, Rahman, MTA, Amin, NAM, Basha, MH, Ismail, MHN & Hamid, AFA 2017, 'Study of intake manifold for Universiti Malaysia Perlis automotive racing team formula student race car', Journal of Physics: Conference Series, vol. 908, p. 012069.

Pogorevc, P & Kegl, B 2006, 'Intake system design procedure for engines with special requirements', Proceedings of the Institution of Mechanical Engineers, Part D: Journal of Automobile Engineering, vol. 220, no. 2, pp. 241–252.

SAE International 2015, 2015 Formula SAE Rules, viewed 24 October 2019, <http://www.fsaeonline.com/content/2015-16%20FSAE%20Rules%20revision%2091714%20kz.pdf>.

Smith, J 2018, When Do I Know My Valvetrain Is In Distress? Tips For Success Here!, EngineLabs, viewed 24 October 2019, <https://www.enginelabs.com/engine-tech/cam-valvetrain/when-do-i-know-my-valvetrain-is-in-distress/>.

Society of Automotive Engineers 2019, Formula SAE Rules, Fsaeonline.com, viewed 7 October 2019, <https://www.fsaeonline.com/cdsweb/gen/DocumentResources.aspx>

14. APPENDICES

14.1 Appendix A –Formula Student & FSAE Rulesets

CV 1.3 Air Intake System

CV 1.3.1 All parts of the engine air and fuel control systems (including the throttle and the complete air intake system, including the air filter and any air boxes) must lie within the surface defined by the top of the roll bar and the outside edge of the four tires. (See Figure 2).

CV 1.3.2 Any portion of the air intake system that is less than 350 mm above the ground must be shielded from side or rear impact collisions by structure built to T 3.15.

CV 1.3.3 The intake manifold must be securely attached to the engine block or cylinder head with brackets and mechanical fasteners. The threaded fasteners used to secure the intake manifold are considered critical fasteners and must comply with T 10.

CV 1.3.4 Intake systems with significant mass or cantilever from the cylinder head must be supported to prevent stress to the intake system. Supports to the engine must be rigid. Supports to the chassis must incorporate isolation to allow for engine movement and chassis torsion.

CV 1.4 Throttle

CV 1.4.1 The vehicle must be equipped with a throttle body. The throttle body may be of any size or design.

CV 1.4.2 The throttle must be actuated mechanically by a foot pedal, i.e. via a cable or a rod system, see CV 1.5, or by an ETC system, see CV 1.6.

CV 1.4.3 Throttle position is defined as percentage of travel from fully closed to fully open where 0 % is fully closed and 100 % is fully open. The idle position is the average position of the throttle body while the engine is idling.

CV 1.4.4 The throttle system mechanism must be protected from debris ingress to prevent jamming.

CV 1.6 Electronic Throttle Control (ETC)

CV 1.6.1 CV 1.6 only applies if ETC is used.

CV 1.6.2 [DV ONLY] Any DV with internal combustion engine is assumed to have ETC.

CV 1.6.3 The team must be able to demonstrate the functionality of all safety features and error detections of the ETC system at technical inspection, see IN.

CV 1.6.4 The ETC system must be equipped with at least the following sensors:

- Accelerator Pedal Position Sensors (APPSs) as defined in T 11.8.
- Two Throttle Position Sensors (TPSs) to measure the throttle position.
- One Brake System Encoder (BSE) to measure brake system pressure to check for plausibility.

CV 1.6.5 All ETC signals are System Critical Signals (SCSs), see T 11.9.

CV 1.6.6 When power is removed, the electronic throttle must immediately close at least to idle position ±5 %. An interval of one second is allowed for the throttle to close to idle, failure to achieve this within the required interval must result in immediate disabling of power to ignition, fuel injectors and fuel pump. This action must remain active until the TPS signals indicate the throttle has returned to idle position ±5 % for at least one second.

CV 1.6.7 If plausibility does not occur between the values of at least two TPSs and this persists for more than 100 ms, the power to the electronic throttle must be immediately shut down. Plausibility is defined as a deviation of less than ten percentage points between the sensor values as defined in CV 1.4.3 and no detected failures as defined in T 11.9.

[DV ONLY] Autonomous system must check this signal consistency on a low level itself.

CV 1.6.8 The electronic throttle must use at least two sources of energy capable of returning the throttle to the closed position. One of the sources may be the device that normally actuates the throttle, e.g. a DC motor, but the other device(s) must be a return spring that can return the throttle to the idle position in the event of a loss of actuator power.

CV 1.6.9 Springs in the TPSs are not acceptable as return springs.

CV 1.6.10 The power to the electronic throttle must be immediately shut down, as defined in CV 1.6.6, if the throttle position differs by more than 10 % from the expected target TPS position for more than 500 ms.

CV 1.6.11 Teams must submit a detailed description of their ETC system not later than the deadline specified in the competition handbook. The document must follow the template layout which is available on the competition website.

CV 1.7 Intake System Restrictor

CV 1.7.1 In order to limit the power capability from the engine(s), a single circular restrictor must be placed in the intake system and all engine(s) airflow must pass through this restrictor. The only allowed sequence of components are the following:

- For naturally aspirated engines, the sequence must be: throttle body, restrictor, and engine, see figure 16
- For turbocharged or supercharged engines, the sequence must be: restrictor, compressor, throttle body, engine, see figure 17

CV 1.7.2 The maximum restrictor diameters which must be respected at all times during the competition are:

- Gasoline fueled vehicles - 20 mm
- E 85 fueled vehicles - 19 mm

CV 1.7.3 The restrictor must be located to facilitate measurement during the inspection process.

CV 1.7.4 The circular restricting cross section may not be movable or flexible in any way, e.g. the restrictor must not be part of the movable portion of a barrel throttle body.

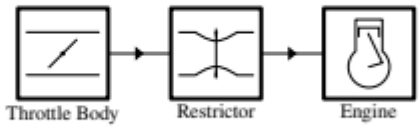

Figure 16: Intake configuration for naturally aspirated engines.

T 11.6 Brake System Plausibility Device (BSPD)

T 11.6.1 A standalone non-programmable circuit, the BSPD, must open the shutdown circuit, see EV 6.1 and CV 4.1, when hard braking occurs, whilst

- [EV ONLY] $\geq$5 kW power is delivered to the motors.
- [CV ONLY] the throttle position is more than 10 % over idle position.

The shutdown circuit must remain open until power cycling the LVMS or the BSPD may reset itself if the opening condition is no longer present for more than 10 s.

T 11.6.2 The action of opening the shutdown circuit must occur if the implausibility is persistent for more than 500 ms.

T 11.6.3 The BSPD must be directly supplied from the LVMS, see T 11.3.

T 11.6.4 Standalone is defined as there is no additional functionality implemented on all required Printed Circuit Boards (PCBs). The interfaces must be reduced to the minimum necessary signals,i.e. power supply, required sensors and the shutdown circuit. Supply and sensor signals must not be routed through any other devices before entering the BSPD.

T 11.6.5 To detect hard braking, a brake system pressure sensor must be used. The threshold must be chosen such that there are no locked wheels and the brake pressure is $\leq$ 30 bar.

T 11.6.6 [EV ONLY] To measure power delivery, a DC circuit current sensor only must be used. The threshold must be chosen to an equivalent of $\leq$5 kW for maximum TS voltage.

T 11.6.7 It must be possible to disconnect each sensor signal wire for technical inspection.

T 11.6.8 All necessary signals are System Critical Signal (SCS), see T 11.9.

T 11.8 Accelerator Pedal Position Sensor (APPS)

T 11.8.1 T 11.8 only apply for electric vehicles, see chapter EV, or internal combustion vehicles using Electronic Throttle Control (ETC), see CV 1.6.

T 11.8.2 The APPS must be actuated by a foot pedal.

T 11.8.3 Pedal travel is defined as percentage of travel from fully released position to a fully applied position where 0 % is fully released and 100 % is fully applied.

T 11.8.4 The foot pedal must return to the 0 % position when not actuated. The foot pedal must have a positive stop preventing the mounted sensors from being damaged or overstressed. Two springs must be used to return the foot pedal to the 0 % position and each spring must work when the other is disconnected. Springs in the APPS are not accepted as return springs.

T 11.8.5 At least two separate sensors must be used as APPSs. Separate is defined as not sharing supply or signal lines.

T 11.8.6 If analog sensors are used, they must have different transfer functions, each having a positive slope sense with either different gradients and/or offsets to the other(s). A short circuit between the signal lines must always result in an implausibility according to T 11.8.9.

T 11.8.7 The APPS signals are SCSs, see T 11.9.

T 11.8.8 If an implausibility occurs between the values of the APPSs and persists for more than 100 ms

- [EV ONLY] The power to the motor(s) must be immediately shut down completely. It is not necessary to completely deactivate the tractive system, the motor controller(s) shutting down the power to the motor(s) is sufficient.
- [CV ONLY] The power to the electronic throttle must be immediately shut down.

T 11.8.9 Implausibility is defined as a deviation of more than ten percentage points pedal travel between any of the used APPSs or any failure according to T 11.9.

T 11.8.10 If three sensors are used, then in the case of an APPS implausibility, any two sensors that are plausible may be used to define the torque target and the 3rd APPS may be ignored.

T 11.8.11 It must be possible to seperately disconnect each APPS signal wire to check all functionalities.

T 11.8.12 A fully released accelerator pedal must result in:

- [EV ONLY] A wheel torque of $\leq 0\,\mathrm{N\,m}$
- [CV ONLY] An idle position or lower throttle set-point. This may only be exceeded during a gearshift for a maximum of 500 ms.

IC.1.2 Air Intake and Fuel System Location

All parts of the engine air system and fuel control, delivery and storage systems (including the throttle or carburetor, and the complete air intake system, including the air cleaner and any air boxes) must lie within the surface defined by the top of the roll bar and the outside edge of the four tires.

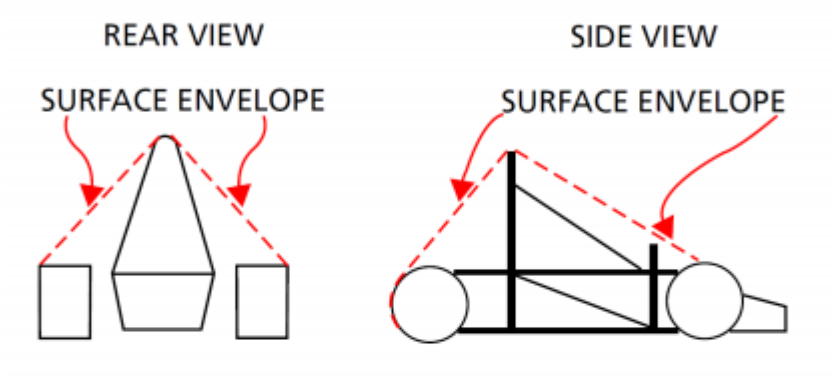

IC.2 AIR INTAKE SYSTEM

IC.2.1 General

IC.2.2 Intake System Location

IC.2.2.1 The Intake System must meet **IC.1.2**

IC.2.2.2 Any portion of the air intake system that is less than 350 mm above the ground must be shielded from side or rear impact collisions by structure built per **T.2.26** / **T.2.34** as applicable.

IC.2.3 Intake System Mounting

IC.2.3.1 The intake manifold must be securely attached to the engine block or cylinder head with brackets and mechanical fasteners. Hose clamps, plastic ties, or safety wires do not meet this requirement.

The use of rubber bushings or hose is acceptable for creating and sealing air passages, but is not a structural attachment.

IC.2.3.2 Threaded fasteners used to secure the intake manifold must have a positive locking feature, see **T.10.3**, or be an OEM fastener.

IC.2.3.3 Intake systems with significant mass or cantilever from the cylinder head must be supported to prevent stress to the intake system.

a. Supports to the engine must be rigid.

b. Supports to the frame or chassis must incorporate some isolation to allow for engine movement and chassis flex.

IC.2.4 Intake System Restrictor

IC.2.4.1 All airflow to the engine(s) must pass through a single circular restrictor placed in the intake system.

IC.2.4.2 The only allowed sequence of components are the following:

a. For naturally aspirated engines, the sequence must be: throttle body, restrictor, and engine.

IC.3 THROTTLE

IC.3.1 General

IC.3.1.1 The vehicle must be equipped with a carburetor or throttle body.

a. The carburetor or throttle body may be of any size or design.

b. Carburetors must not be used on boosted applications.

IC.3.1.2 The foot pedal must return to its original position when not actuated

IC.3.1.3 A positive pedal stop must be incorporated on the throttle pedal to prevent over stressing the throttle cable or actuation system.

IC.3.1.4 If the throttle system contains any mechanism that could become jammed, for example a gear mechanism, then this must be covered to prevent ingress of any debris.

IC.3.2 Throttle Actuation Method

IC.3.2.1 The throttle may be actuated either mechanically by a cable or rod system, or by Electronic Throttle Control.

IC.4 ELECTRONIC THROTTLE CONTROL

This section IC.4 applies only when Electronic Throttle Control is used

An Electronic Throttle Control (ETC) system may be used. This is a device or system which may change the engine throttle setting based on various inputs.

IC.4.1 General Design

IC.4.1.1 The electronic throttle must automatically close (return to idle) when power is removed.

IC.4.1.2 The electronic throttle must use at least two sources of energy capable of returning the throttle to the idle position.

a. One of the sources may be the device (such as a DC motor) that normally actuates the throttle

b. The other device(s) must be a throttle return spring that can return the throttle to the idle position in the event of a loss of actuator power.

c. Springs in the TPS are not acceptable throttle return springs

IC.4.1.3 The ETC system may blip the throttle during downshifts when the control strategy and its possible failure modes, including all signals used to determine that the driveline state is open and unable to transmit propulsive torque when the blipping function is active are properly documented in the FMEA and demonstrated at Technical Inspection.

IC.4.2 Commercial ETC System

IC.4.2.1 An ETC system that is commercially available, but does not comply with the regulations, may be used, if approved prior to the event.

IC.4.2.2 To obtain approval, submit a Rules Question which includes:

- Which ETC system the team is seeking approval to use.
- The specific ETC rule(s) that the commercial system deviates from.
- Sufficient technical details of these deviations to allow the acceptability of the commercial system to be determined.

IC.4.3 Documentation

IC.4.3.1 The ETC Notice of Intent:

- Must be submitted to inform the organizer of the intent to run ETC
- May be used to screen which teams are allowed to use ETC

IC.4.3.2 The Failure Modes and Effects Analysis – FMEA must be submitted in order to use ETC

IC.4.3.3 Submit the ETC Notice of Intent and ETC - FMEA as described in section **DR - Document Requirements**

IC.4.3.4 Late or non submission will prevent use of ETC, see **DR.3.4**

IC.4.4 Throttle Position Sensor - TPS

IC.4.4.1 The TPS must measure the position of the throttle or the throttle actuator.

Throttle position is defined as percent of travel from fully closed to wide open where 0% is fully closed and 100% is fully open.

IC.4.4.2 At least two separate sensors must be used as TPSs. The TPSs may share the same supply and reference lines only if effects of supply and/or reference line voltage offsets can be detected.

IC.4.4.3 Implausibility is defined as a deviation of more than 10% throttle position between the sensors or other failure as defined in Section **IC.4**. Use of larger values may be considered on a case by case basis and require justification in the FMEA.

IC.4.4.4 If an implausibility occurs between the values of the two TPSs and persists for more than 100 msec, the power to the electronic throttle must be immediately shut down.

IC.4.4.5 If three sensors are used, then in the case of a TPS failure, any two TPSs that agree within 10% throttle position may be used to define the throttle position target and the 3rd TPS may be ignored.

IC.4.4.6 Each TPS must be able to be checked during Technical Inspection by having either:

a. A separate detachable connector that enables a check of these functions by unplugging it
b. An inline switchable breakout box available that allows disconnection of each TPS signal.

IC.4.4.7 The TPS signals must be sent directly to the throttle controller using an analogue signal or via a digital data transmission bus such as CAN or FlexRay. Any failure of the TPSs or TPS wiring must be detectable by the controller and must be treated like implausibility.

IC.4.4.8 When an analogue signal is used, the TPSs will be considered to have failed when they achieve an open circuit or short circuit condition which generates a signal outside of the normal operating range, for example <0.5 V or >4.5 V. The circuitry used to evaluate the sensor must use pull down or pull up resistors to ensure that open circuit signals result in a failure being detected.

IC.4.4.9 When any kind of digital data transmission is used to transmit the TPS signal,

a. The FMEA study must contain a detailed description of all the potential failure modes that can occur, the strategy that is used to detect these failures and the tests that have been conducted to prove that the detection strategy works.
b. The failures to be considered must include but are not limited to the failure of the TPS, TPS signals being out of range, corruption of the message and loss of messages and the associated time outs.

IC.4.5 Accelerator Pedal Position Sensor - APPS

Refer to **T.6.2** for specific requirements of the APPS

IC.4.6 Brake System Encoder - BSE

Refer to **T.6.3** for specific requirements of the BSE

IC.4.7 Plausibility Checks

IC.4.7.1 Brakes and Throttle Position

a. The power to the electronic throttle must be shut down if the mechanical brakes are actuated and the TPS signals that the throttle is open by more than a permitted amount for more than one second.

b. An interval of one second is allowed for the throttle to close (return to idle). Failure to achieve this within the required interval must result in immediate shut down of fuel flow and the ignition system.

c. The permitted relationship between BSE and TPS may be defined by the team using a table, but the functionality must be demonstrated at Technical Inspection.

IC.4.7.2 Throttle Position vs Target

a. The power to the electronic throttle must be immediately shut down, if throttle position differs by more than 10% from the expected target TPS position for more than one second.

b. An interval of one second is allowed for the difference to reduce to less than 10%, failure to achieve this within the required interval must result in immediate shut down of fuel flow and the ignition system.

c. An error in TPS position and the resultant system shutdown must be demonstrated at Technical Inspection.

IC.4.7.3 The electronic throttle and fuel injector/ignition system shutdown must remain active until the TPS signals indicate the throttle is at or below the unpowered default position for at least one second.

IC.4.8 Brake System Plausibility Device (BSPD)

IC.4.8.1 A standalone nonprogrammable circuit must be used that will check for any of the following conditions:

a. Both of the following for more than one second:

- Hard braking (for example >0.8 g deceleration but without locking the wheels)
- Throttle greater than 10% open

b. Loss of signal from the braking sensor(s)

c. Loss of signal from the throttle sensor(s)

d. Removal of power from the BSPD circuit

IC.4.8.2 When any of the above conditions exist, the following must happen:

- Shut off power to the electronic throttle
- Shut off fuel flow
- Close the throttle to the idle position

IC.4.8.3 The BSPD may only be reset by power cycling the Primary Master Switch.

IC.4.8.4 This device must be provided in addition to the plausibility checks which are carried out in the ETC which interprets the drivers throttle request and controls the engine throttle position.

IC.4.8.5 The team must devise a test to prove these required functions during Technical Inspection.

T.6 ELECTRONIC THROTTLE COMPONENTS

T.6.1 Applicability

This section applies only for:

- IC vehicles using Electronic Throttle Control (ETC)
- EV vehicles

Differences between IC and EV applications are noted in the rule text

T.6.2 Accelerator Pedal Position Sensor - APPS

T.6.2.1 The APPS must be actuated by a foot pedal.

a. Pedal travel is defined as percent of travel from a fully released position to a fully applied position where 0% is fully released and 100% is fully applied.

b. The foot pedal must return to its original position when not actuated.

c. The foot pedal must have a positive stop preventing the mounted sensors from being damaged or overstressed.

d. Two springs must be used to return the foot pedal to the off position

e. Each spring must be capable of returning the pedal to the fully released position with the other disconnected. The springs in the APPS are not acceptable pedal return springs.

T.6.2.2 At least two entirely separate sensors have to be used as APPSs. The sensors must have different transfer functions which meet either:

- Each sensor has a positive slope sense with either different gradients and/or offsets to the other(s).
- An OEM pedal sensor with opposite slopes. Non OEM opposite slope sensor configurations require prior approval.

The intent is that in a short circuit the APPSs will only agree at 0% pedal position.

T.6.2.3 Implausibility is defined as a deviation of more than 10% pedal travel between the sensors or other failure as defined in this Section T.6.2. Use of values larger than 10% require justification in the FMEA and may not be approved

T.6.2.4 If an implausibility occurs between the values of the APPSs and persists for more than 100msec, the power to the (IC) electronic throttle / (EV) motor(s) must be immediately shut down completely.

(EV only) It is not necessary to completely deactivate the Tractive System, the motor controller(s) shutting down the power to the motor(s) is sufficient.

T.6.2.5 If three sensors are used, then in the case of an APPS failure, any two sensors that agree within 10% pedal travel may be used to define the (IC) throttle position / (EV) torque target and the 3rd APPS may be ignored.

T.6.2.6 Each APPS must be able to be checked during Technical Inspection by having either:

- A separate detachable connector that enables a check of functions by unplugging it
- An inline switchable breakout box available that allows disconnection of each APPS signal.

T.6.2.7 The APPS signals must be sent directly to a controller using an analogue signal or via a digital data transmission bus such as CAN or FlexRay.

T.6.2.8 Any failure of the APPS or APPS wiring must be detectable by the controller and must be treated like an implausibility, see **T.6.2.3 above**

T.6.2.9 When an analogue signal is used, the APPS will be considered to have failed when they achieve an open circuit or short circuit condition which generates a signal outside of the normal operating range, for example <0.5 V or >4.5 V.

The circuitry used to evaluate the sensor must use pull down or pull up resistors to ensure that open circuit signals result in a failure being detected.

T.6.2.10 When any kind of digital data transmission is used to transmit the APPS signal,

a. The FMEA study must contain a detailed description of all the potential failure modes that can occur, the strategy that is used to detect these failures and the tests that have been conducted to prove that the detection strategy works.

b. The failures to be considered must include but are not limited to the failure of the APPS, APPS signals being out of range, corruption of the message and loss of messages and the associated time outs.

T.6.2.11 The current rules are written to only apply to the APPS (pedal), but the integrity of the torque command signal is important in all stages.

14.2 Appendix B – Technical Drawings

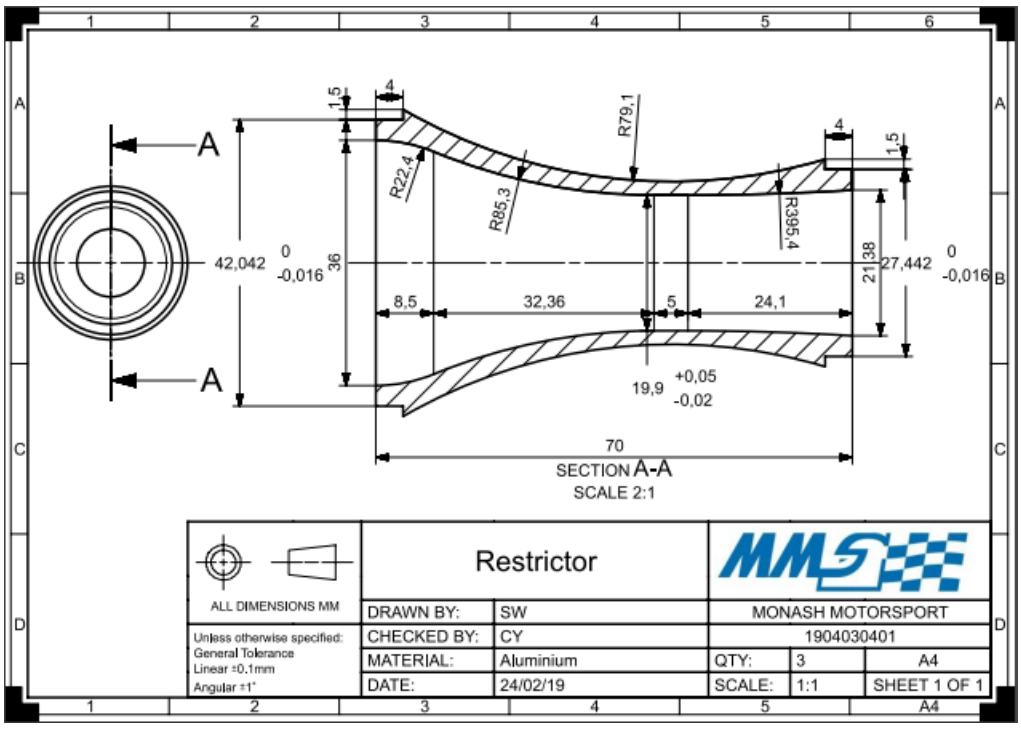

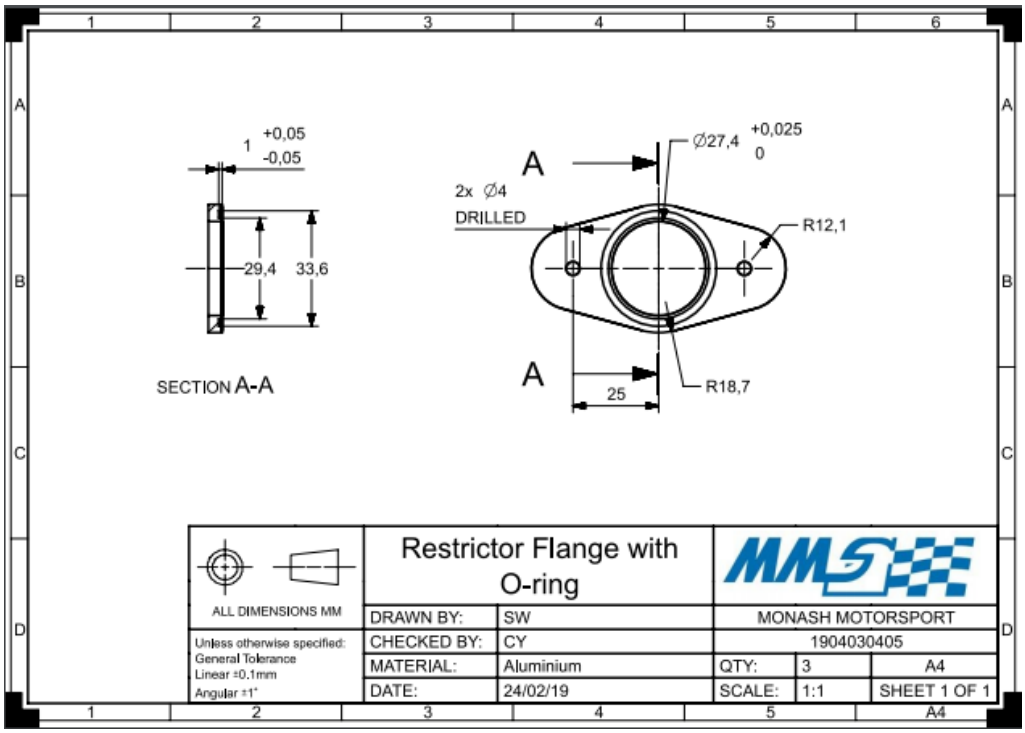

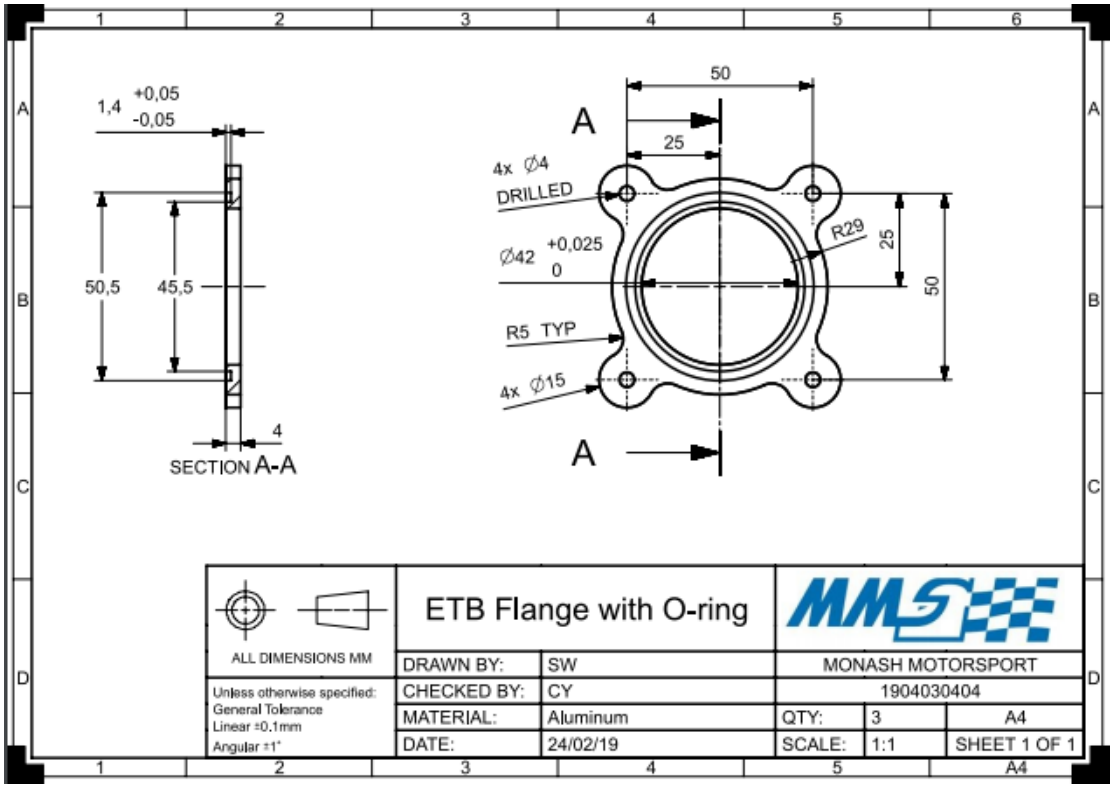
1,4 +0,05 -0,05
50,5
45,5
4
SECTION A-A
A
50
25
4x Ø4
DRILLED
Ø42 +0,025 0
R29
25
50
R5 TYP
4x Ø15
A
ETB Flange with O-ring
ALL DIMENSIONS MM
Unless otherwise specified:
General Tolerance
Linear ±0.1mm
Angular ±1°
DRAWN BY: SW
CHECKED BY: CY
MATERIAL: Aluminum
DATE: 24/02/19
MONASH MOTORSPORT
1904030404
QTY: 3
SCALE: 1:1
A4
SHEET 1 OF 1

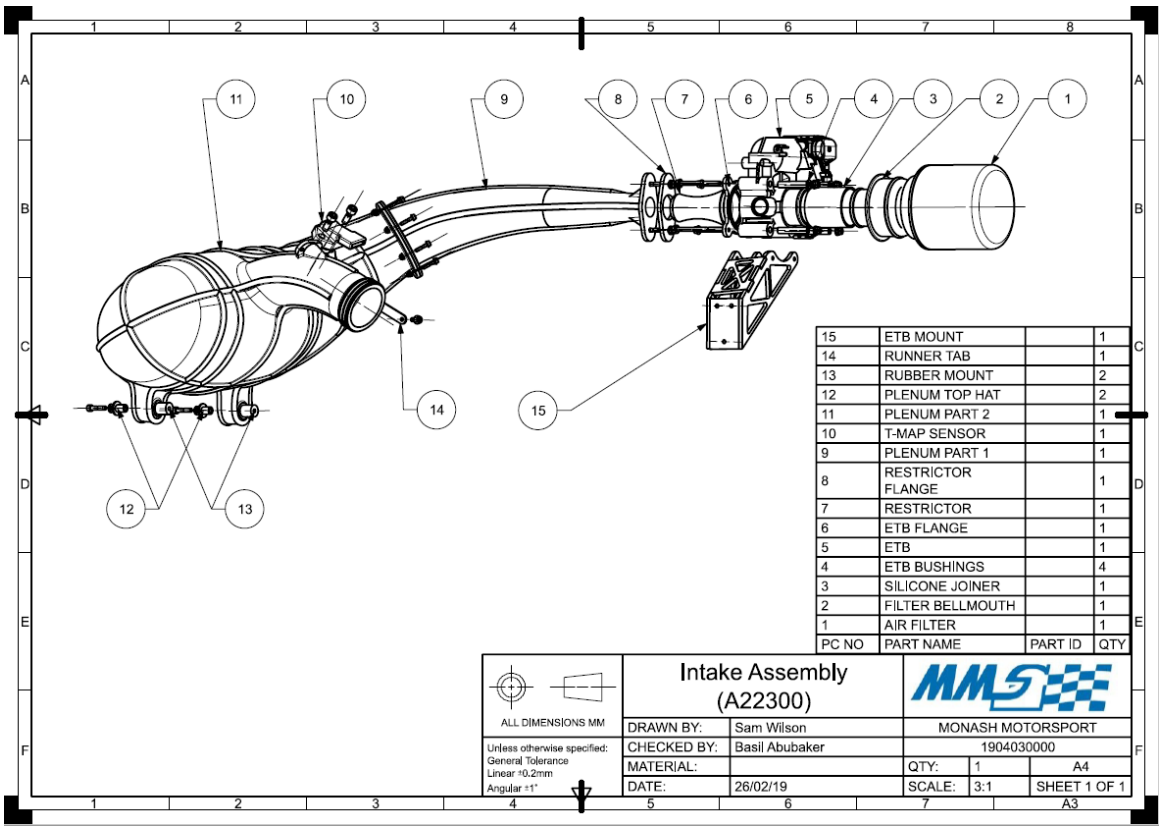
11
10
9
8
7
6
5
4
3
2
1
12
13
14
15
15 ETB MOUNT 1
14 RUNNER TAB 1
13 RUBBER MOUNT 2
12 PLENUM TOP HAT 2
11 PLENUM PART 2 1
10 T-MAP SENSOR 1
9 PLENUM PART 1 1
8 RESTRICTOR FLANGE 1
7 RESTRICTOR 1
6 ETB FLANGE 1
5 ETB 1
4 ETB BUSHINGS 4
3 SILICONE JOINER 1
2 FILTER BELLMOUTH 1
1 AIR FILTER 1
PC NO PART NAME PART ID QTY
Intake Assembly
(A22300)
ALL DIMENSIONS MM
Unless otherwise specified:
General Tolerance
Linear ±0.2mm
Angular ±1°
DRAWN BY: Sam Wilson
CHECKED BY: Basil Abubaker
MATERIAL:
DATE: 26/02/19
MONASH MOTORSPORT
1904030000
QTY: 1
SCALE: 3:1
A4
SHEET 1 OF 1
A3

14.3 Appendix C – FEA Setup

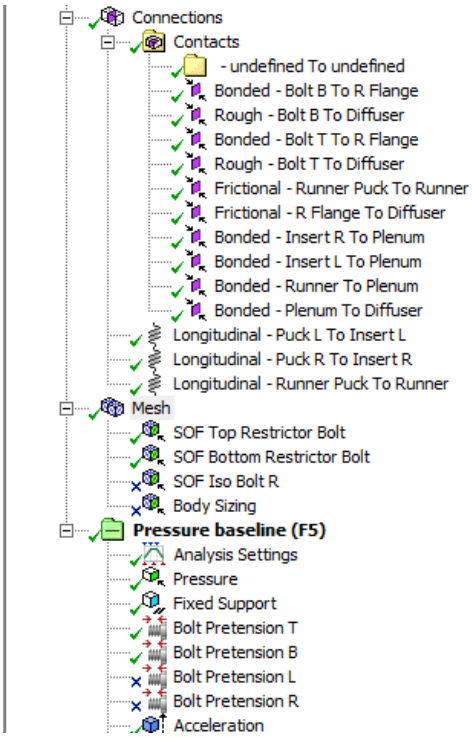

Contacts, constraints and mesh setup.

Properties of Outline Row 9: Nylon 12 GF new

	A	B	C	D	E
1	Property	Value	Unit		
2	Material Field Variables	Table			
3	Density	1.49	g cm^-3		
4	Isotropic Elasticity				
5	Derive from	Young's Modulus and Po...			
6	Young's Modulus	2400	MPa		
7	Poisson's Ratio	0.35			
8	Bulk Modulus	2.6667E+09	Pa		
9	Shear Modulus	8.8889E+08	Pa		
10	Tensile Yield Strength	25	MPa		
11	Tensile Ultimate Strength	24	MPa		

Final material setup within ANSYS, after calibration to physical data,

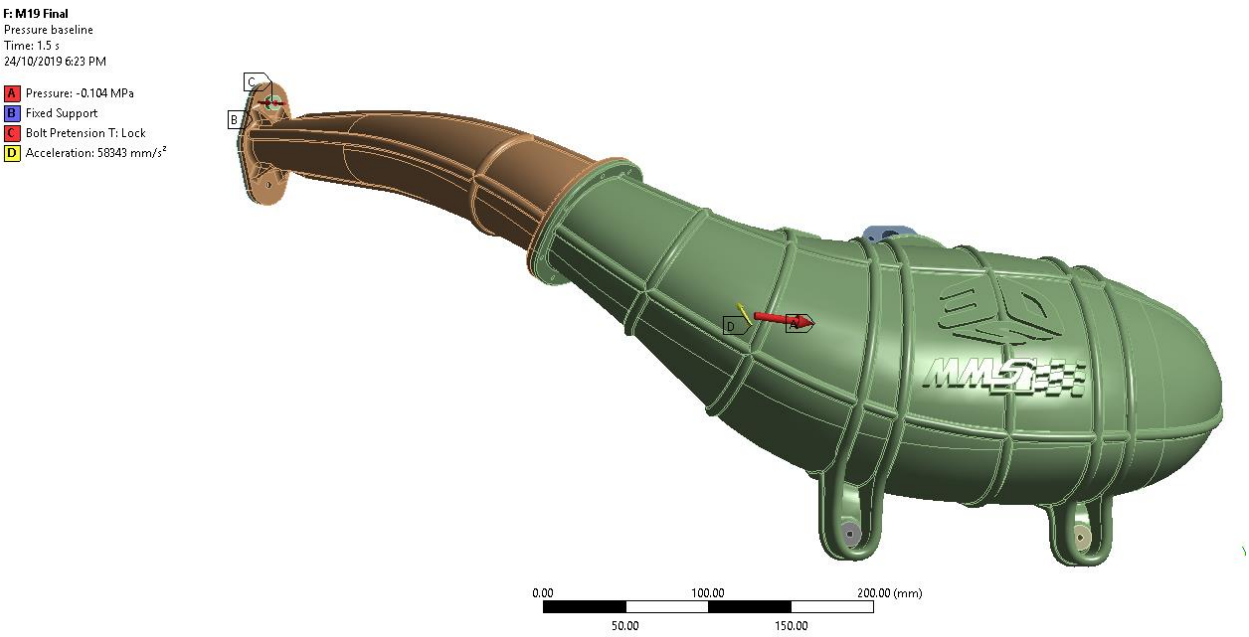
F: M19 Final
Pressure baseline
Time: 1.5 s
24/10/2019 6:23 PM
A Pressure: -0.104 MPa
B Fixed Support
C Bolt Pretension T: Lock
D Acceleration: 58343 mm/s²
0.00
100.00
200.00 (mm)
50.00
150.00

14.4 Appendix D – CFD Setup

Area	Setting	Value (sizes in mm)
General Mesh Settings	Element Size	3
	Maximum Element Size	50
	Growth Rate	1.2
Wall Face Sizing	Element Size	3
	Growth Rate	1.2
Wall Inflation	Method	First Layer Height
	Method Control	0.003
	Number of Layers	30
	Growth Rate	1.2
Butterfly Valve Face Sizing	Element Size	0.25
	Growth Rate	1.1

Area	Setting	Value
Boundary Conditions	Pressure Inlet	0 Pa (gauge pressure)
	Mass-Flow Outlet	0.0583 kg/s
	Non-Slip Wall	
Turbulence Model	k-ω SST	
	Curvature Correction	
Solver	Pressure Based Coupled Solver	
	Pseudo-Transient	
	Timescale Factor	0.05
	Iterations	1000